การดัดแปรขั้วไฟฟ้าคาร์บอนด้วยเส้นใยอิเล็กโทรสปันแกรฟีน/พอลิแอนิลีน
สำหรับการตรวจวัดตะกั่วและแคดเมียม

นางสาวนาฏตินันทร์ พรหมเพชร

วิทยานิพนธ์นี้เป็นส่วนหนึ่งของการศึกษาตามหลักสูตรปริญญาวิทยาศาสตรมหาบัณฑิต
สาขาวิชาปิโตรเคมีและวิทยาศาสตร์พอลิเมอร์
คณะวิทยาศาสตร์ จุฬาลงกรณ์มหาวิทยาลัย
ปีการศึกษา 2557

MODIFICATION OF CARBON ELECTRODE WITH GRAPHENE/POLYANILINE ELECTROSPUN FIBERS FOR LEAD AND CADMIUM DETECTION

Miss Nadtinan Promphet

A Thesis Submitted in Partial Fulfillment of the Requirements
for the Degree of Master of Science Program in Petrochemistry and Polymer Science
Faculty of Science
Chulalongkorn University
Academic Year 2014

Thesis Title	MODIFICATION OF CARBON ELECTRODE WITH GRAPHENE/POLYANILINE ELECTROSPUN FIBERS FOR LEAD AND CADMIUM DETECTION
By	Miss Nadtinan Promphet
Field of Study	Petrochemistry and Polymer Science
Thesis Advisor	Professor Orawon Chailapakul, Ph.D.
Thesis Co-Advisor	Nadnudda Rodthongkum, Ph.D.
	Ratthapol Rangkupan, Ph.D.

Accepted by the Faculty of Science, Chulalongkorn University in Partial Fulfillment of the Requirements for the Master's Degree

.....Dean of the Faculty of Science
(Professor Supot Hannongbua, Dr.rer.nat.)

THESIS COMMITTEE

.....Chairman
(Assistant Professor Warinthorn Chavasiri, Ph.D.)

.....Thesis Advisor
(Professor Orawon Chailapakul, Ph.D.)

.....Thesis Co-Advisor
(Nadnudda Rodthongkum, Ph.D.)

.....Thesis Co-Advisor
(Ratthapol Rangkupan, Ph.D.)

.....Examiner
(Associate Professor Nuanphun Chantarasiri, Ph.D.)

.....External Examiner
(Assistant Professor Weena Siangproh, Ph.D.)

นาฏตินันทร์ พรหมเพชร : การดัดแปรขั้วไฟฟ้าคาร์บอนด้วยเส้นใยอิเล็กโทรสปันแกรฟีน/พอลิแอนิลีนสำหรับการตรวจวัดตะกั่วและแคดเมียม (MODIFICATION OF CARBON ELECTRODE WITH GRAPHENE/POLYANILINE ELECTROSPUN FIBERS FOR LEAD AND CADMIUM DETECTION) อ.ที่ปรึกษาวิทยานิพนธ์หลัก: ศ. ดร.อรวรรณ ชัยลภากุล, อ.ที่ปรึกษาวิทยานิพนธ์ร่วม: ดร.นาฏนัดดา รอดทองคำ, ดร.รัฐพล รังกุพันธุ์, 63 หน้า.

งานวิจัยนี้ได้ดัดแปรขั้วไฟฟ้าคาร์บอนด้วยเส้นใยอิเล็กโทรสปันที่มีรูพรุนขนาดนาโนของแกรฟีน/พอลิแอนิลีน/พอลิสไตรีน โดยใช้วิธีการปั่นเส้นใยด้วยไฟฟ้าสถิตสำหรับตรวจวัดตะกั่วและแคดเมียม ในงานวิจัยนี้ได้ศึกษาหาภาวะที่เหมาะสมและปัจจัยที่ควบคุมลักษณะทางสันฐานวิทยาและความไวในการตรวจวัดทางเคมีไฟฟ้าของเส้นใยอิเล็กโทรสปันที่มีรูพรุนขนาดนาโนของแกรฟีน/พอลิแอนิลีน/พอลิสไตรีน เช่น ระบบของตัวทำละลาย ชนิดของพอลิเมอร์ตัวพา ปริมาณของแกรฟีน เป็นต้น โดยศึกษาลักษณะทางสัณฐานวิทยาของเส้นใยอิเล็กโทรสปันที่มีรูพรุนขนาดนาโนของแกรฟีน/พอลิแอนิลีน/พอลิสไตรีน ด้วยกล้องจุลทรรศน์อิเล็กตรอนแบบส่องกราดและกล้องจุลทรรศน์อิเล็กตรอนแบบส่องผ่าน พบว่าระบบของตัวทำละลายเป็นปัจจัยสำคัญ ที่ส่งผลต่อลักษณะทางสัณฐานวิทยาของเส้นใยอิเล็กโทรสปันที่มีรูพรุนของแกรฟีน/พอลิแอนิลีน/พอลิสไตรีน สำหรับความสามารถในการตรวจวัดทางเคมีไฟฟ้าศึกษาด้วยสารมาตรฐานเฟอริ/เฟอโรไซยาไนด์โดยใช้เทคนิคไซคลิกโวลแทมเมตรี พบว่าขั้วไฟฟ้าที่ดัดแปรด้วยเส้นใยอิเล็กโทรสปันที่มีรูพรุนขนาดนาโนของแกรฟีน/พอลิแอนิลีน/พอลิสไตรีน มีกระแสตอบสนองสูงกว่าขั้วไฟฟ้าที่ไม่ได้ดัดแปรถึง 3 เท่า ในด้านการประยุกต์ใช้งานขั้วไฟฟ้าที่ดัดแปรนี้ถูกนำมาใช้สำหรับการตรวจวัดตะกั่วและแคดเมียมพร้อมกัน โดยใช้เทคนิคสแควร์เวฟแอโนดิกสทริปปิงโวลแทมเมตรีร่วมกับการเคลือบเกาะของบิสมัท ภายใต้สภาวะที่เหมาะสมพบว่าความสัมพันธ์เชิงเส้นตรงระหว่างความเข้มข้นกับสัญญาณอยู่ในช่วงความเข้มข้น 10-500 ไมโครกรัมต่อลิตรสำหรับทั้งตะกั่วและแคดเมียม สำหรับขีดจำกัดการตรวจวัด (S/N=3) ของระบบนี้คือ 3.30 ไมโครกรัมต่อลิตรสำหรับตะกั่ว และ 4.43 ไมโครกรัมต่อลิตรสำหรับแคดเมียม อีกทั้งขั้วไฟฟ้าที่ดัดแปรสามารถนำกลับมาใช้ซ้ำได้อย่างน้อย 10 ครั้ง นอกจากนี้ระบบของขั้วไฟฟ้าที่ดัดแปรนี้ถูกนำไปใช้ในการตรวจวัดตะกั่วและแคดเมียมในแม่น้ำ ซึ่งผลที่ได้สอดคล้องกับผลที่ได้จากเทคนิคอินดักทีฟลีคัพเพิลพลาสมาออพติคอลอิมิสชันสเปกโทรเมตรี

สาขาวิชา ปิโตรเคมีและวิทยาศาสตร์พอลิเมอร์ ลายมือชื่อนิสิต .....

ปีการศึกษา 2557 ลายมือชื่อ อ.ที่ปรึกษาหลัก .....

ลายมือชื่อ อ.ที่ปรึกษาร่วม .....

ลายมือชื่อ อ.ที่ปรึกษาร่วม .....

5472255323 : MAJOR PETROCHEMISTRY AND POLYMER SCIENCE
KEYWORDS: GRAPHENE / POLYANILINE / NANOPOROUS FIBERS / ELECTROSPINNING / LEAD / CADMIUM

NADTINAN PROMPHET: MODIFICATION OF CARBON ELECTRODE WITH GRAPHENE/POLYANILINE ELECTROSPUN FIBERS FOR LEAD AND CADMIUM DETECTION. ADVISOR: PROF. ORAWON CHAILAPAKUL, Ph.D., CO-ADVISOR: NADNUDDA RODTHONGKUM, Ph.D., RATTHAPOL RANGKUPAN, Ph.D., 63 pp.

The nanoporous fibers of graphene/polyaniline/polystyrene (G/PANI/PS) were fabricated on carbon electrode by electrospinning for the determination of lead (Pb^{2+}) and cadmium (Cd^{2+}). In this study, the parameters controlling the morphology and electrochemical sensitivity of the electrospun G/PANI/PS nanoporous fiber electrodes, such as solvent system, type of carrier polymer and amount of G loading were investigated and optimized. The electrospun G/PANI/PS nanoporous fiber morphology was characterized by scanning electron microscopy (SEM) and transmission electron microscopy (TEM). The results showed that solvent system was the most important factor affecting the morphology of the electrospun G/PANI/PS nanoporous fibers. The electrochemical sensitivity of the modified electrode was investigated by cyclic voltammetry (CV) using a standard ferri/ferrocyanide [$Fe(CN_6)^{3-/4-}$] redox couple. The current response of electrospun G/PANI/PS nanoporous fibers was higher than unmodified carbon electrode approximately 3 folds. In term of application, the modified electrode was applied for simultaneous Pb^{2+} and Cd^{2+} in the presence of bismuth (Bi^{3+}) with square wave anodic stripping voltammetry (SWASV). Under the optimized condition, a linear relationship was found in a range of 10-500 μg L^{-1} of both Pb^{2+} and Cd^{2+}. The detection limit (S/N=3) was obtained at 3.30 μg L^{-1} and 4.43 μg L^{-1} for Pb^{2+} and Cd^{2+}, respectively. Furthermore, the modified electrode can be reused for more than ten replicates. This system was successfully applied for the simultaneous determination of Pb^{2+} and Cd^{2+} in river water samples, and the results correlate well with the obtained from conventional inductively coupled plasma optical emission spectroscopy (ICP-OES).

Field of Study:	Petrochemistry and Polymer Science	Student's Signature	.....
		Advisor's Signature	.....
Academic Year:	2014	Co-Advisor's Signature	.....
		Co-Advisor's Signature	.....

ACKNOWLEDGEMENTS

I would like to thank to my thesis advisor and co-advisors, Professor Dr. Orawon Chailapakul, Dr. Nadnudda Rodthongkum and Dr. Ratthapol Rangkupan for their support and advice on this thesis.

I am thankful to all the committee members, Assistant Professor Dr. Warinthorn Chavasiri, Associate Professor Dr. Nuanphun Chantarasiri and Assistant Professor Dr. Weena Siangproh for their comment and suggestion.

I am grateful to the financial supports from the Thailand Research Fund (TRF), through the New Researchers Grant (TRG5680012), the National Research University Project, Office of Higher Education Commission (WCU-026-AM-57), and the National Nanotechnology Center (NANOTEC), NSTDA, Ministry of Science and Technology, Thailand through its program of Center of Excellence Network.

In addition, I am grateful to all members of my researcher group for their kindness and great friendship.

Finally, I would like to thank my family for their love and support throughout my life.

CONTENTS

Page

Page

Page

Page

LIST OF TABLES

Table **Page**

LIST OF FIGURES

Figure **Page**

CHAPTER I
INTRODUCTION

1.1 Introduction

Electrochemical detection is a versatile technique for various fields of applications such as food inspection, clinical diagnosis and environmental monitoring because it is simple, rapid, portable and inexpensive [1, 2]. Normally, the working electrode of electrochemical sensor is designed to be a small size to provide the portability for on-site analysis and the compatibility with trace amount of sample. The small size of electrode significantly decreases the sensitivity of electrochemical detection. Therefore, electrode surface modification becomes a crucial step to enhance the electrochemical sensitivity.

Various materials in nanoscopic scale have been used for electrode surface modification such as metallic nanoparticles [3-6] and carbon based nanomaterials (*e.g.* fullerene, carbon nanotube, graphene) [7, 8]. In the recent year, graphene (G), a two-dimensional single atom thick of carbon material, has become a material of interest for electrode surface modification due to its outstanding electrical conductivity, mechanical strength and large surface area. However, the pure form of G agglomerates easily to form of graphite [9, 10]. To prevent G agglomeration, conducting polymers are used to improve G distribution on the electrode surface. Several conducting polymers including polyaniline (PANI) [11-19], polypyrrole (PPy) [20-22], poly (3, 4-ethylenedioxythiophene) (PEDOT) [23-25] have been used to prepare the well-dispersed G onto the electrode surface. Among all, PANI is an attractive conducting polymer because of its high conductivity, good environment stability, and easily controllable properties [11, 19]. Previously, it has been reported that G and PANI nanocomposite possesses a high tendency to improve the electrochemical sensitivity and analytical performance of electrochemical sensor [13-15, 17, 26].

For the modification of G/PANI nanocomposite on electrochemical sensor, electrospinning technique is selected because it is a very useful technique which is developed to cost-effectively produce continuous polymer fibers with diameter in the range of nanometer (nm) to micrometer (μm). In addition, the morphology of nanofibers can be controlled by changing the parameters in the spinning process such as concentration of polymer, solvent system, electric field strength and humidity [27, 28]. Electrospun fibers with different size and shape have been prepared, such as ribbon, core shell, hollow, smooth and porous fibers [29, 30]. In the process, continuous fibers are generated by applying high voltage electric field to the polymer solution or melt, and then nanofibers are produced at the collector. The main advantages of electrospun nanofibers for electrochemical sensor are large specific surface area, high porosity, and high mechanical property [29]. Among all morphologies, the nanoporous fiber has received more attention for electrochemical sensor due to its ultra-high specific surface area leading to enhanced electrochemical sensitivity in electrochemical detection [4, 14, 31-34]. Furthermore, the stability and life time of the electrochemical sensor modified by electrospun fiber are significantly improved compared to an unmodified electrode [31, 32].

For the environmental pollutants, heavy metals are serious concern due to their wide applications in industrial processes (*e.g.* electroplating, batteries, paint). Particularly, lead (Pb^{2+}) and cadmium (Cd^{2+}) are two highly toxic heavy metals because of their non-biodegradability. Moreover, they can accumulate in the human body, causing disorder of human organs (*e.g.* kidneys liver, central nervous system, bone) [35]. Several analytical techniques have been used for heavy metals detection, such as atomic adsorption spectrometry (AAS) [36, 37], inductively couple plasma optical mass spectrometry (ICP-MS) [38, 39], X-ray fluorescence spectroscopy (XRF) [40]. However, these techniques require expensive instruments, specialized operator, and long analysis time [8]. In contrast, the electrochemical related techniques offer several advantages including fast analysis, low operating cost, portability and high sensitivity [41]. Anodic stripping voltammetry (ASV) using the square-wave pulse form (SWASV) has been established as a highly sensitive

electrochemical method for the trace metal ion analysis due to incorporation of two procedures consisting of deposition and the measurement step [42]. In the deposition step, the potential is held at a lower potential to accumulate the metal of interest onto the electrode surface in the presence of bismuth ion (Bi^{3+}). The metal-bismuth alloy form on electrode surface was introduced as an environmental friendly modifier since it offers high sensitivity, well-defined peaks and highly reproducible stripping signals [2, 12, 43-46].

Herein, electrospun nanoporous fibers of G/PANI/PS nanocomposite were prepared and used for electrochemical sensor modification. G/PANI/PS nanoporous fibers were modified on electrode surface to enhance the electrochemical sensitivity for the simultaneous determination of Pb^{2+} and Cd^{2+} and then applied to detect Pb^{2+} and Cd^{2+} in environmental sample (*i.e.* river water).

1.2 Objective

- To prepare electrospun nanoporous fibers of G/PANI/PS via electrospinning.

- To modify electrochemical sensor using G/PANI/PS nanoporous fibers and use them for the silmultaneous determination of Pb^{2+} and Cd^{2+}.

- To apply G/PANI/PS nanoporous fibers modified electrochemical sensor for the detection of Pb^{2+} and Cd^{2+} in environmental sample.

1.3 Scope of the thesis

In this study, nanocomposites of graphene (G), polyaniline (PANI) and polystyrene (PS) were prepared by physical mixing. The obtained nanocomposites were used to modify the electrode surface via electrospinning and applied for electrochemical detection of heavy metal ions (*e.g.* Pb^{2+} and Cd^{2+}). Fabrication parameters, including type of solvent, amount of G loading, type of carrier polymer were investigated and optimized. The optimized G/PANI/PS nanoporous fibers modified electrode was used for the determination of Pb^{2+} and Cd^{2+} in river water.

CHAPTER II
THEORY AND LITERATURE SURVEY

In this chapter, definitions and basic principle for understanding in electrochemical analysis are explained. The materials used for electrode modification, such as graphene, polyaniline and techniques used for electrode modification (*i.e.* electrospinning technique) are discussed. Finally, the target analytes including lead and cadmium are introduced.

2.1 Electrochemical analysis

Electrochemical detection is an important and sensitive analytical technique for both qualitative and quantitative analysis. This technique is based on oxidation and reduction process of the electro active species. Two types of electroanalytical measurements are potentiometric and potentiostatic. The potentiometric technique is a static (zero current) technique, which measures accumulation of a charge potential between two electrodes (working and reference electrode) in an electrochemical cell. These techniques may be used for direct monitoring of ionic species and determination of analyte concentration. For the potentiostatic or controlled potential techniques (*e.g.* voltammetry, amperometry, coulometry), it is a dynamic technique (no zero current), which measures the current response from an electron-transfer reaction when the potential is applied to an electrochemical cell [47]. Although many methods of electrochemical analysis are available, only voltammetric methods including cyclic voltammetry and anodic stripping voltammetry are used in this thesis.

2.1.1 Cyclic voltammetry

Cyclic voltammetry (CV) is the most widely used technique in electrochemical analysis for initial study of electrochemical reactions of new system. The information obtained from this technique are thermodynamic of redox processes, kinetic of electron transfer reactions and couple chemical reactions or adsorption processes.

In the cyclic voltammetry, the voltage is applied to the working electrode with the triangular waveform (Figure 2.1a). The triangular waveform is the potential sweep

in a negative potential direction (reduction reaction, $O + ne^- \leftrightharpoons R$) and when it reaches a switching potential (E_λ), the sweep potential is reversed in a positive direction (oxidation reaction, $R \leftrightharpoons O + ne^-$). The output of cyclic voltammetry plot of current versus potential is called cyclic voltammogram (Figure 2.1b).

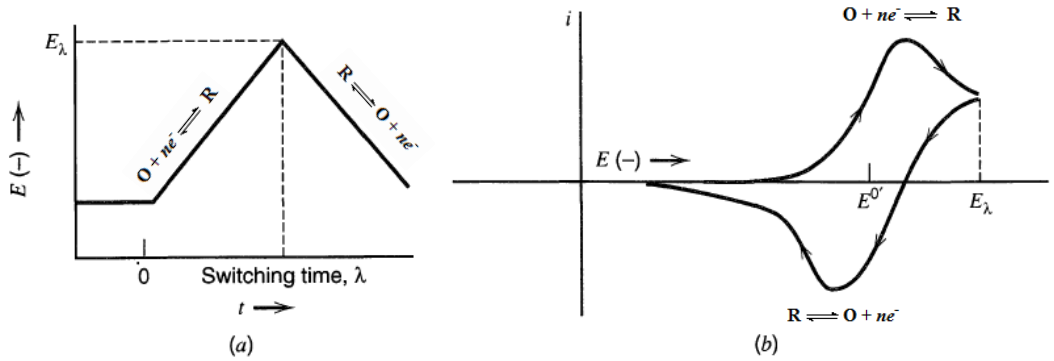

Figure 2.1 Cyclic potential sweep (triangular waveform) (a) and cyclic voltammogram of a reversible redox process (b) [48].

The cyclic voltammogram is characterized by peak potential (E_p) and peak current (I_p) for redox process. The peak current for a reversible redox couple (at 25 °C) is given by Randles-Sevcik equation:

$$i_p = (2.69 \times 10^5)\, n^{3/2} A C D^{1/2} \nu^{1/2} \qquad \text{(equation 2.1)}$$

Where n is the number of transferred electrons, A is the electrode surface area (cm^2), C is the concentration of the electroactive species (mol cm^{-3}), D is the diffusion coefficient ($cm^2\ s^{-1}$), and ν is the scan rate ($V\ s^{-1}$) [47, 49].

2.1.2 Anodic stripping voltammetry

Stripping voltammetry is the most sensitive electrochemical analysis technique for metals detection because it consist of a preconcentration step in the measurement procedures. The step of stripping voltammetry is divided into two parts. The first, deposition or preconcentration step, the negative potential is applied for accumulation metal targets as a metallic form onto the surface of working electrode to preconcentrate metal analytes. Then, stripping step is followed by scanning the potential in a positive direction to reoxidize the metallic form into the solution and

detect the current signals that proportional to the analyte concentration. In stripping step, the peak potential can be used to identify the type of metal [47, 49]. The sequence of potential-time for using in anodic stripping voltammetry and the resulting of stripping voltammogram are shown in Figure 2.2.

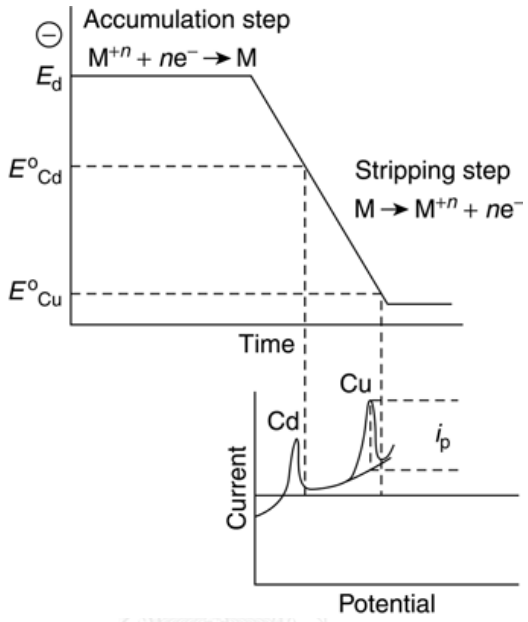

Figure 2.2 Anodic stripping voltammetry; the potential time waveform (top) with the resulting voltammogram (bottom) [47].

In the voltammetric measurement, an electrochemical cell consists of three electrode system (working electrode, reference electrode and auxiliary or counter electrode), that immerses in the sample solution (Figure 2.3). The reaction of interest takes place at the working electrode surface. The electrode, which has a stable and constant (reversible) potential, is called a reference electrode and the counter is used to provide a complete electric circuit in an electrochemical cell.

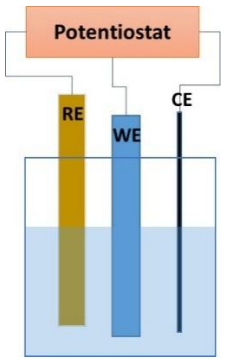

Figure 2.3 Schematic diagram of electrochemical cell for voltammetric measurement: WE, working electrode; RE, reference electrode; CE, counter electrode.

2.1.3 Electrode surface modification

Electrochemical sensor consists three electrode system including reference, counter and working electrode. For the detection of analyte, working electrode is the most important part because its performance directly affect the sensitivity of the system for analyte determination. To improve the sensitivity of electrochemical sensor, various types of materials such as nanocarbon (*e.g.* fullerene, carbon nanotube, graphene) and conducting polymers (*i.e.* polyaniline) are used to modify the surface of working electrode surface.

2.1.3.1 Nanocarbon materials

Carbon based nanomaterials such as carbon nanotube, carbon nanofiber, graphite, fullerene and graphene have been used for electrode surface modification due to the high specific surface area leading to increase the sensitivity and electron transfer of electrode. However, carbon nanotubes can be contaminated with metal particles in synthesis process. These problems can affect the accuracy and precision in the measurement of analytes. Recently, graphene was discovered and it was used for electrode surface modification instead of carbon nanotubes because the problems associated with carbon nanotube were eliminated [7].

Graphene (G) is a two-dimensional (2D) single atom thick of carbon nanomaterials. Graphene has become a material of interest for electrode modification due to its remarkable properties, including high specific surface area of 2600 m^2 g^{-1},

excellent thermal conductivity of 5000 W m^{-1} K^{-1}, high-speed electron mobility of 200000 cm^2 V^{-1} s^{-1} at room temperature, high stiffness and strength with Young's modulus of around 1000 GPa and break strength of 130 GPa, extraordinary electrocatalytic activity, optical properties and electrochemical properties [7, 50, 51].

2.1.3.2 Polyaniline

Various conducting polymers such as polyaniline (PANI), polypyrrole (PPy), and poly(3,4-ethylenedioxythiophene) (PEDOT) have been used to improve the sensitivity of electrochemical sensor. Among all, PANI is one of the most interesting conducting polymer due to its high conductivity, good environmental stability and tunable properties. PANI has highly electrical conductivity in a range of 1 to 100 S cm^{-1}. It has three basis different structures including fully reduced leucoemeraldine base (LEB), fully oxidized pernigraniline base (PNB) and half oxidized/half reduced emeraldine base (EB) state depending on the oxidation state as shown in (Figure 2.4). The conjugate **π** electron system and electron delocalization in PANI structure provide a high conductivity that occur by protonation or doping polyaniline emeraldine base to form of emeraldine salt (Figure 2.5), while leucoemeraldine base and pernigraniline base protonation are insulating in nature [11, 52].

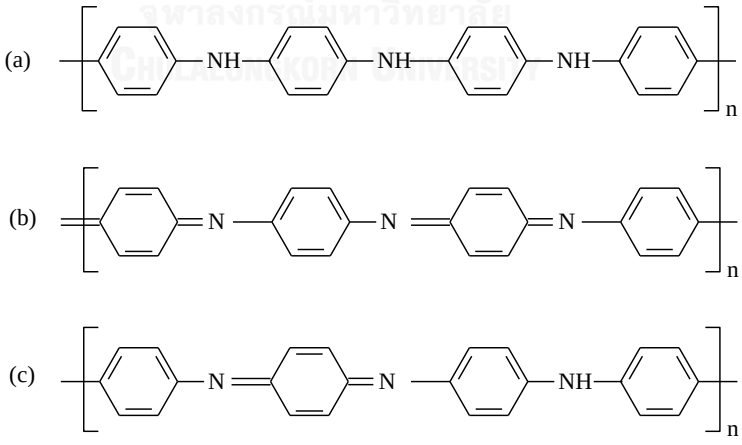

Figure 2.4 The three oxidation states of polyaniline: (a) a fully reduced leucoemeraldine base (LEB); (b) a fully oxidized pernigraniline base (PNB); and (c) a half oxidized/half reduced emeraldine base (EB) state.

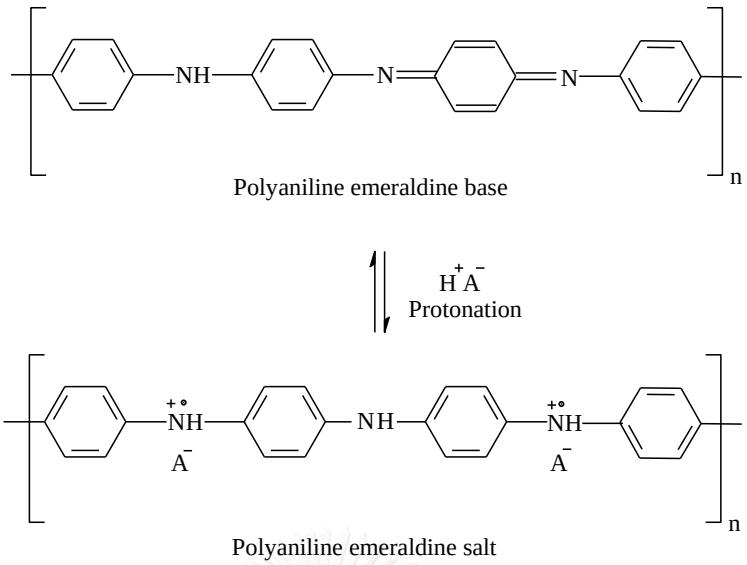

Figure 2.5 The protonation of polyaniline emeraldine base to polyaniline emeraldine salt.

Nanocomposite of graphene and conducting polymer, such as polyaniline, poly (3, 4-ethylenedioxythiophene): polystyrene sulfonic acid show a potential application in electrochemical sensor. Many researchers have been used these nanocomposite for electrode modification to enhance the electrode conductivity.

Wang *et al.* [17] reported a novel polyaniline nanofibers (PANI-NF) based electrochemical sensor for specific detection of nitrile and sensitive monitoring of ascorbic acid scavenging nitrile. The PANI-NF sensor showed a fast response time, high sensitivity, wide linear range, low detection limit and excellent stability.

Xue *et al.* [53] prepared aniline into microporous polyacrylonitrile-coated platinum electrode by electropolymerization for glucose determination. This novel glucose sensor exhibited a high selectivity, sensitivity and stability. The glucose biosensor was applied blood glucose determination and showed a close correlation with hospital laboratory.

Wisitsoraat *et al*. [24] developed graphene-poly (3, 4-ethylenedioxythiophene): polystyrene sulfonic acid (G-PEDOT:PSS) nanocomposite by drop-coated on screen-printed carbon electrode and then glucose oxidase (GOD) enzyme was immobilized

using glutaraldehyde as a crosslinking agent. This glucose biosensor showed a high sensitivity and good stability for glucose detection.

Fan *et al.* [13] prepared graphene-polyaniline (G-PANI) composite film modified glassy carbon electrode for 4-aminophenol determination. This G-PANI composite film modified GCE provided a low detection limit, high sensitivity, long term stability, and can be used for simultaneous determination of 4-aminophenol and paracetamol.

Ruecha *et al.* [15] developed graphene/polyvinylpyrrolidone/polyaniline (G/PVP/PANI) nanocomposite on paper based electrochemical sensor for cholesterol determination. The G/PVP/PANI modified electrode exhibited a high-sensitivity, wide linear range and low limit of detection for cholesterol.

For electrospun nanofibers modification, the composite of graphene and conducting polymers is difficult to produce because it has a low viscosity. Therefore, it need to be blended with other polymers to increase the viscosity (*e.g.* polystyrene, polyamide, poly(vinyl alcohol), poly(ethylene oxide)) [16, 54].

2.1.3.3 Polystyrene

Polystyrene (PS) is one of the most wildly used commercial polymer due to low cost, good electric and excellent mechanical property [55]. Polystyrene is an amorphous polymer containing a long chain hydrocarbon with a phenyl group (Figure 2.6) and it can produce by free radical polymerization from styrene monomer.

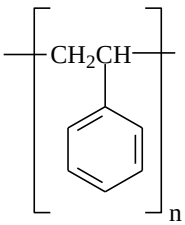

Figure 2.6 The structure of polystyrene.

In general, non-conducting polymer such as polystyrene is mixed with the conductive part and then used for electrode modification because the non-conducting polymer can assist the nanofiber fabrication process and stabilizing the conductive part.

Khaskheli *et al.* [56] prepared micro-crystalline nature graphite-polystyrene composite modified electrode for paracetamol determination. The sensor was successfully used for the determination of paacetamol in pharmaceutical formulations and human urine. The limit of determination was found to be 0.034 mol L^{-1}.

Qian *et al.* [57] prepared gold nanoparticles coated polystyrene/reduce graphite oxide composite for electrode modification. The sensor exhibits excellent sensitivity and selectivity for dopamine detection.

Xu *et al.* [55] fabricated carbon nanotube/polystyrene composite electrode by in situ polymerization of mixed carbon nanotube/polystyrene in the end of column microchip capillary electrophoresis for separation and detection of rutin and quercetin. This sensor shows the high resolution and sensitivity for rutin and quercetin.

2.1.3.4 Bismuth film

In heavy metal detection, mercury electrodes have been used for anodic stripping voltammetry (ASV) to obtain high sensitivity; however, mercury is highly toxic. Bismuth film electrode has been introduced as an environmental friendly modifier because it offers high sensitivity, well-defined peak shape and highly reproducible stripping signal [2, 12, 43-46]. The attractive behavior of bismuth electrode is attributed to form a fusible alloys (binary or multicomponent) with heavy metal at the preconcentration step:

$$Bi^{3+} + 3e^{-} \longrightarrow Bi^{0} \qquad \text{(equation 2.2)}$$

$$M^{n+} + ne^{-} \longrightarrow M(Bi) \qquad \text{(equation 2.3)}$$

Normally, there are three methods for bismuth coating on the electrode surface. The first method is preplating or ex-situ plating, the bismuth film ions are prepared before transferring the electrode to the analyte solution. The second

method is in-situ plating, the method is added directly bismuth ions into the analyte solution and during measurement the bismuth film is simultaneously deposited with the metal analyte on the surface of electrode. Generally, the concentration of bismuth must be 10-fold higher than the analyte concentration to avoid saturation effect. The third method is the modification of electrode based on bismuth precursor [58-60].

In this study, the in-situ plating of bismuth ions is used for lead and cadmium detection due to its simple preparation.

Several researchers have been used in-situ bismuth for electrode modification to improve the electrochemical sensitivity for heavy metal determination.

Wonsawat *et al.* [61] developed graphene-carbon paste electrode combined with bismuth for lead and cadmium detection in a flow based system. In this system, in-situ bismuth was used to modify electrode to improve the electrochemical sensitivity in the determination of lead and cadmium. This system showed the increased surface area and excellent electrical conductivity. The modified electrode was successfully applied to detect lead and cadmium in the complex samples with a low detection limit.

Chen *et al.* [12] modified glassy carbon electrode with bismuth/nafion/thiolate polyaniline for lead and cadmium determination. The proposed sensor exhibited a high sensitivity with detection limit of 0.05 μg L^{-1} for Pb^{2+} and 0.04 μg L^{-1} for Cd^{2+}.

Chen *et al.* [44] fabricated disposable bismuth-coated porous screen-printed carbon electrode by in-situ electrodeposition of bismuth for trace lead and cadmium determination. This modified electrode demonstrated the enhanced sensitivity for lead and cadmium detection. In addition, this electrode was easy to prepare and low coat.

2.2 Fabrication technique

The fibers with diameter in the range of nano to micrometer scale provide several advantages such as high specific surface-to-volume ratio, high porosity, and high mechanical properties [29]. The high specific surface area is important for various applications including electrochemical sensor, enzyme immobilization, tissue

engineering and filtration [28, 62]. Various processing techniques can be used for ultrafine-fiber fabrication such as mechanical drawing, template synthesis, self-assembly, phase separation and electrospinning [63]. Among these, electrospinning is one of the most versatile and cost-effective technique to produce ultrafine-fibers.

2.2.1 Electrospinning process

Electrospinning is a method of interest due to its low cost and simple set up for producing a continuous fibers [16]. Electrospinning is derived from "electrostatic spinning". This technique creates continuous fibers with a diameter in a range from nanometer to micrometer based on electrohydrodynamic process [27]. Three important components of electrospinning set up are high voltage DC power supply, polymer reservoir with spinneret, and fiber collecting device. In usual, set up the high voltage side of the high power supplied is connected to the spinneret, while the ground electrode is connected to a fiber collecting device as shown in figrure2.7. In the process, a surface of polymer liquid, either solution or melt, is charged by high voltage electric fields. Due to Coulombic repulsion among surface charges at sufficient electrical field strength, the liquid surface deformed and self-ejected from the spinneret to form a continuous stream of charged polymer jet. Subsequently, elongation via electrically-driven begin instability and solidification of the jet lead to a formation of ultrafine droplets or nanofibers [64, 65].

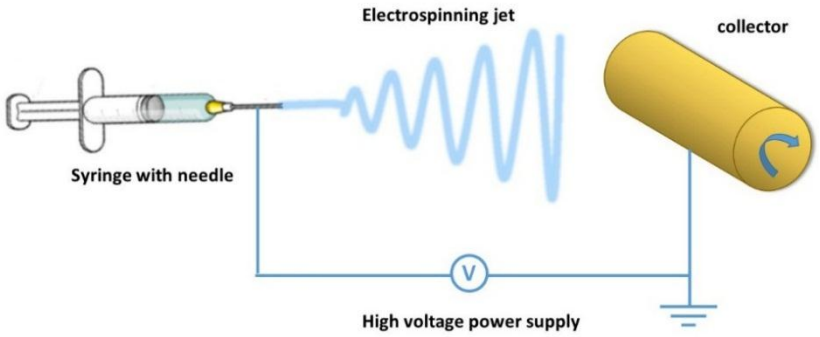

Figure 2.7 Schematic set up of horizontal electrospinning apparatus.

The electrospinning process can be divided into 3 steps: Initiation, elongation and solidification of charged jet [66]. In the first step, the initiation of polymer charged jet as shown in Figure 2.8, a polymer liquid is pumped at low flow rate into a spinneret. Polymer solution is extruded from the spinneret tip and forms a hemispherical droplet (stage 1). The electric charged at the surface of polymer droplet is induced upon applying high voltage electric field where the positive charge species migrate to the droplet surface (stage 2). As the applied electric field increased the surface is deform in to a cone-like shape called "Taylor cone" (stage 3). Above the critical voltage, when the repulsive force is able to overcome the surface tension of liquid polymer, a charged jet is ejected from the needle tip (stage 4).

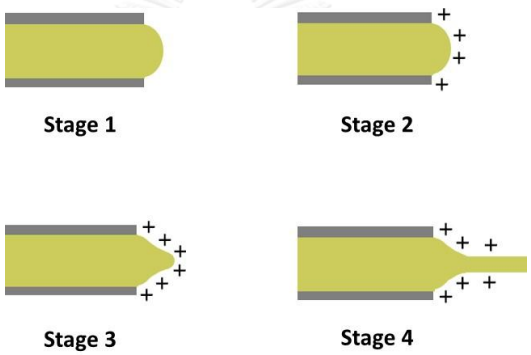

Figure 2.8 Diagram of charge jet initiation in the electrospinning process [67].

Once the charged jet is created, the jet undergo the elongation. The Coulombic repulsion among surface charges on the jet is the dominant force that cause the segment of the jet to elongate. As the jet segment elongates and move towards the collector, the diameter of jet decreases rapidly due to both extension and evaporation of solvent.

The termination step of electrospinning process is solidification of charge jet into the fiber on the collector due to the rate of solvent evaporation. The solidification rate varies with the polymer concentration, electrostatic field and gap distance [68].

2.2.2 Effect of electrospinning parameter on fiber size and morphology

The size and morphology of electrospun fibers can be controlled by the electrospinning parameters, such as polymer concentration, solvent type, applied

voltage, flow rate and spinneret configuration [27]. Figure 2.9 shows the different morphology of fibers produced from electrospinning, such as ribbon, core shell, hollow, smooth and porous fibers [29, 30].

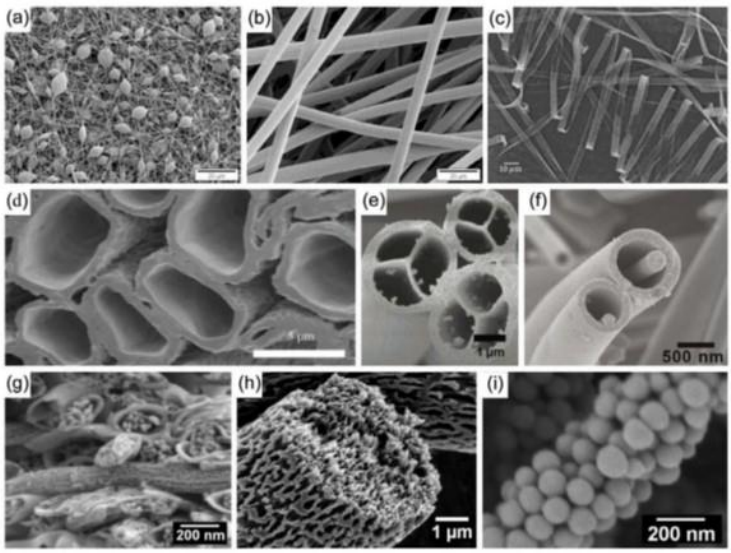

Figure 2.9 Different morphologies of electrospun fibers: (a) beaded; (b) smooth; (c) ribbon; (d) hollow; (e) multichannel tubular; (f) nanowire-in-microtube; (g) multi-core cable-like and (h,i) porous fibers [30].

Electrospinning parameters can be divided into three groups: solution parameter, process parameter and ambient parameter.

2.2.2.1 Solution parameters

The solution concentration plays an important role in the formation of electrospun fibers since it relates to solution viscosity, and hence, molecular entanglement of polymer chains in the solution. By increasing the concentration of polymer solution, the solution viscosity increases due to higher entanglement of polymer chains. Insufficient chain entanglement, at very dilute or low concentration solution, particles or beaded fibers are formed. Increasing concentration allows polymer chains in the charged jet enough entanglement to prevent jet break up from surface tension effect resulting in disappearance of bead formation [29, 69, 70].

Solvent system for electrospinning is one of the most important factor for electrospinning since solvent properties, such as dielectric constant, surface tension and vapor pressure (or boiling point) can affect size, morphology, uniformity, and spinnability or processability of polymer solutions of choice [71]. For example, vapor pressure or volatility of solvent can be used to create nanostructure on the fibers to form porous fibers, or as shown in Figure 2.10, change in solvent boiling point can be used to manipulate fibers diameter.

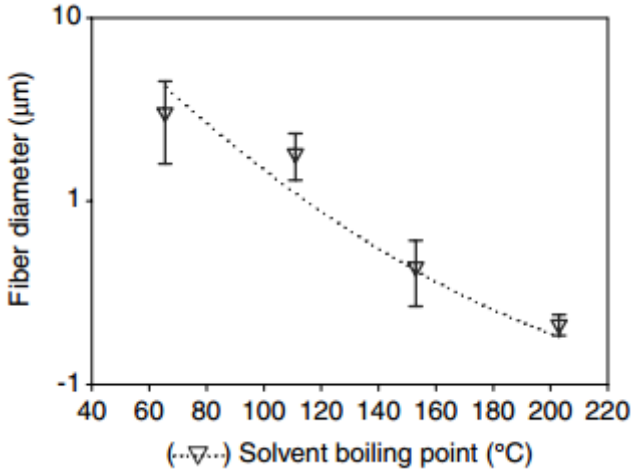

Figure 2.10 The relationship between the boiling point and average fiber diameter in electrospinning of polystyrene from solution in solvent of different boiling points [72].

2.2.2.2 Process parameters

The important parameters of electrospinning process that affect to the morphology of fibers including applied voltage potential, flow rate and distance between needle tip to collector will be discussed.

The influence of applied voltage potential to the polymer solution is a main important parameter for electrospinning because it is the only driving force that induces surface charged onto the polymer droplet, which later become the charged jet. In general, higher applied voltages resulted in higher electric field strength and higher number of charges to be induced on the surface of polymer jet, and thus, higher Coulombic's repulsive force among surface charges. The effect of applied voltage on the average diameter of fibers is shown in Figure 2.11, where increasing applied voltage

produces thinner fibers because the high voltage causes greater stretching of solutions. However, changing applied voltage also affect volumetric mass flow rate of the jet at fiber spinning spot, which would reverse the trend we discuss here. Furthermore, the increasing in applied high voltage increases the deposition rate on the collector because of a high mass flow rate from needle tip [29, 69, 70].

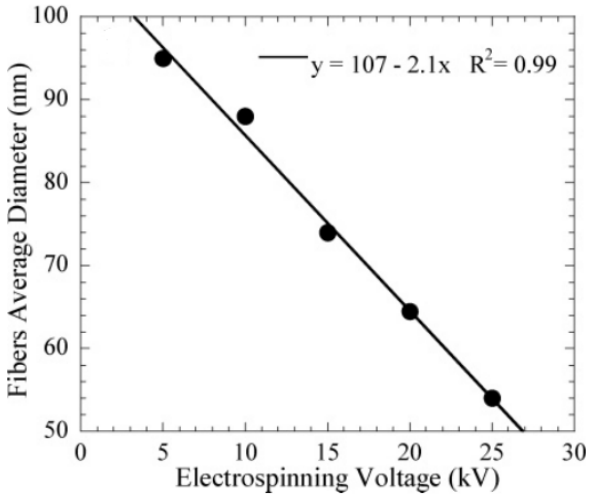

Figure 2.11 The effect of applied voltage on average fiber diameter of poly(acrylonitrile) (PAN)/carbon nanotube (CNT)/titanium dioxide (TiO_2) electrospun fiber in dimetylformamide (DMF) solution [73].

Distance between spinneret to collector is a space that allow fiber segment to elongate and solidify. Too close of a distance will hinder the charged jet from elongation to its fullest extension possible at a given process parameter leading to a large fiber formation. Too short of a distance will also limit solvent evaporation of the charged jet resulting in wet fibers that fused together when dry, as shown in Figure 2.12.

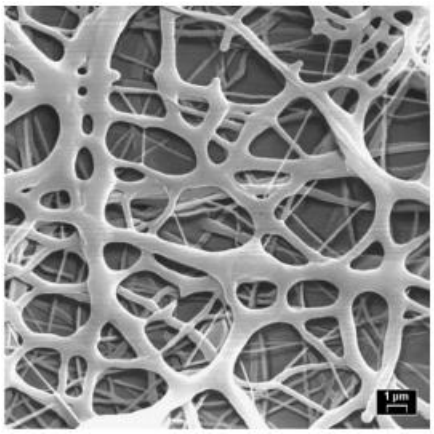

Figure 2.12 Electrospun of poly(**ε**-caprolactone) in form fused wet fibers [74].

2.2.2.3 Environment parameters

Environment parameters (*e.g.* temperature, humidity) influence on the fiber structure and morphology of electrospun fibers. The fiber diameter decreases with increasing in temperature because of the viscosity of the polymer solutions decreases. The humidity affect to the porosity on electrospun fiber. The porosity on the electrospun fibers surface increases when increasing the humidity because the moisture in the air condenses on the fiber surface [29, 70].

2.3 Electrospinning applications in electrochemical sensors

Many researchers have been used electrospinning technique for fabricating the composite for electrochemical sensor applications, because electrospun fiber can increased the surface area of working electrode, leading to enhance electrochemical sensitivity.

Marx et al. [31] reported gold nanofiber modified electrochemical sensor for fructose detection that can increase the surface area for high enzymes immobilization and enhance electrochemical sensitivity. This modified electrode could enhance the efficiency of enzymes loading higher than conventional flat gold disc electrode for 8 fold and can be used with high stability over 20 cycles of use.

Sundaray *et al.* [16] prepared polyaniline-polyethylene oxide nanofibers with single-wall carbon nanotube (PANI-PEO/SWNT) by electrospinning. The PANI-

PEO/SWNT nanofibers demonstrated highly conducting and can be used for highly efficiency for battery electrodes.

Shin *et al.* [75] fabricated multi-walled carbon nanotubes (MWCNT) and polyaniline (PANI) /poly(ethylene oxide) (PEO) composite nanofibers via electrospinning technique. The composite enhances the electrical property.

Scampicchio et al. [32] introduced a novel glucose biosensors by immobilization of glucose oxidase on electrospun nylon nanofibers. This novel biosensor shows high sensitivity, long life time and excellent reproducibility for glucose detecion.

Rodthongkum *et al.* [14] developed electrochemical sensor for dopamine determination based on graphene (G)/polyaniline (PANI)/ polystyrene (PS) nanofibers via electrospinning. The modified electrode shows high sensitivity, good selectivity and wide linear range for dopamine detection.

For sensor application, the porous fibers are more attractive than other fiber morphologies because porous fibers contain with ultra-high specific surface area. Many researchers have been used electrospinning technique for controlling the morphology of electrospun porous fibers.

Casper *et al*. [76] investigated the effect of humidity and molecular weight of polystyrene on the surface of electrospun fiber. The pore diameter and the pore size distribution increase when the amount of humidity increase, and a pore size of fibers increase with increasing the molecular weight of polymer.

Megelski *et al*. [77] investigated the parameters (*e.g.* solvent volatility, concentration of polymer, voltage, flow rate) affecting the pore formation on the electrospun fibers. The results showed that the pore formation on the fiber was created by rapid solvent evaporation. Thus, the property of solvent plays an important role on the pore formation of electrospun fibers.

Fashandi *et al*. [28] investigated the pore formation on both surface and interior fiber morphology on the polystyrene electrospun fiber using *N, N*-dimethylformamide (DMF) and tetrahydrofuran (THF) as a mixed solvent. The H_2O/DMF/PS and H_2O/THF/PS

as the solvent systems were used in the study. The pore are created within the fiber for DMF system and the pore are created on the fiber surface for THF system. The pore formation process of polymer solution undergoing penetration of water from gaseous phase are called vapor-induced phase separation (VIPS). Moreover, they reported that the humidity and temperature of electrospinning process affect the morphology of electrospun fibers (*i.e.* non-porous, porous and wrinkled).

Yu *et al*. [62] prepared polyacrylonitrile (PAN) porous fibers by electrospinning a ternary system of PAN/ *N, N*-dimethylformamide (DMF)/water (H_2O). The porous fibers are generated by non-solvent in the system induced phase separation of the solution. The Brunauer-Emmett-Teller (BET) was used to measure the surface area of fibers, 3 fold increases in surface area was achieved with PAN porous fiber and nonporous PAN fiber.

2.4 Heavy metals

Heavy metal is metallic element with high density and poisonous even at low concentration. Especially, lead (Pb^{2+}) and cadmium (Cd^{2+}) are major serious concern pollution in the environmental and they are harmful to human health. Lead and cadmium are mainly produced from industry of lead acid batteries, solder, alloy, cable sheathing, pigment and rust inhibitors. These toxic heavy metals can cause the disorder to human organ system such as the hematological system, the central nervous system, the renal system and kidneys system [35, 78, 79]. For detection of lead and cadmium by electrochemistry, they can be directly electrochemical detection by reduction reaction as followed;

$$Pb^{2+}(aq) + 2e^- \longrightarrow Pb(s) \qquad \text{(equation 2.4)}$$

$$Cd^{2+}(aq) + 2e^- \longrightarrow Cd(s) \qquad \text{(equation 2.5)}$$

Many researchers have been used an electrochemical analysis (*i.e.* anodic stripping voltammetry) for heavy metal detection.

Guell *et al.* [43] reported screen-printed carbon electrode with square wave anodic stripping voltammetry for the detection of lead and cadmium in seawater. This

modified electrode showed an improved sensitivity with a wide linear range (10-2000 μg L^{-1}) and low detection limit (1.8 μg L^{-1} for Pb^{2+} and 2.9 μg L^{-1} for Cd^{2+}).

Yantasee *et al.* [1] developed a composite of thiol self-assemble monolayer on mesoporous support and Nafion on glassy carbon electrode along with square wave anodic stripping voltammetry for cadmium, lead and copper detection. The developed sensor can be used for simultaneous detection of Cd^{2+}, Pb^{2+} and Cu^{2+} in non-pretreated samples. This sensor showed good electrochemical sensitivity with the detection limits of 2.5 μg L^{-1} of Cd^{2+}, Pb^{2+} and Cu^{2+} and exhibited long service time.

Lv *et al.* [41] prepared an electrochemical sensor based on cyclodextrin-reduce graphene oxide hybrid nanosheets for the detection of lead and cadmium by square wave anodic stripping voltammetry. This sensor demonstrated high sensitivity, good stability and high reproducibility.

Wang [10] prepared ultrathin film electrode modified with bismuth nanoparticle and polyaniline porous layers for lead and cadmium determination using square wave anodic stripping voltammetry. The modified electrode showed high sensitivity and excellent repeatability.

CHAPTER III

EXPERIMENTAL

3.1 Chemicals and reagents

3.1.1 Graphene (G) nanopowders (SkySpring Nanomaterials Inc, Houston, TX, USA)

3.1.2 Polyaniline (PANI) emeraldine base (Mw of 65,000) (Sigma-Aldrich, St. Louis, Mo, USA)

3.1.3 (+)-Camphor-10-sulfonic acid (CSA) (Sigma-Aldrich, St. Louis, Mo, USA)

3.1.4 Polystyrene (PS) (Mw of 180,000) (Sigma-Aldrich, St. Louis, Mo, USA)

3.1.5 Potassium ferricyanide ($K_3[Fe(CN_6)]$) (Sigma-Aldrich, St. Louis, Mo, USA)

3.1.6 Potassium ferrocyanide ($K_4[Fe(CN_6)]$) (Sigma-Aldrich, St. Louis, Mo, USA)

3.1.7 Potassium chloride (KCl) (PFCL Ltd., New Deli, India)

3.1.8 Chloroform ($CHCl_3$) (Carlo Erba reagent, Milano, Italy)

3.1.9 *N, N*-dimethylformamide (DMF) (Carlo Erba reagent, Milano, Italy)

3.1.10 Tetrahydrofuran (THF) (Carlo Erba reagent, Milano, Italy)

3.1.11 Hydrochloric acid (HCl) (Carlo Erba reagent, Milano, Italy)

3.1.12 Bismuth (Bi^{3+}) 1000 mgL^{-1} standard solution (VWR International Ltd., Poole, England)

3.1.13 Cadmium (Cd^{2+}) 1000 mgL^{-1} standard solution (VWR International Ltd., Poole, England)

3.1.14 Lead (Pb^{2+}) 1000 mgL^{-1} standard solution (VWR International Ltd., Poole, England)

3.2 Instrument and equipment

3.2.1 Syringe pump (New Era Pumps, NE300, USA)

3.2.2 High voltage DC module (Gamma High voltage, model UC5-30P/CM/ VM (3), Florida, USA)

3.2.3 Scanning electron microscope (Japan Electron Optics Laboratory Co., Ltd., Japan)

3.2.4 Transmission electron microscope (Hitachi/ s-4800)

3.2.5 Brunauer–Emmett–Teller analysis (Quantachrome/Autosorb-1, Thermo Finnigan/Sortomatic 1990)

3.2.6 μAUTOLAB type III potentiostat (Metrohm Siam Company Ltd.)

3.3 Preparation of solutions

All aqueous solutions were prepared in Mili-Q water (12.8 MΩ cm). All chemicals were used as received without further purification.

3.3.1 Preparation of 0.5 M Potassium chloride solution

Potassium chloride solution (KCl) was used as supporting electrolyte of a standard ferri/ferro cyanide $[Fe(CN)_6]^{3-/4-}$ redox couple. 0.5 M KCl was prepared by dissolving KCl (9.32 g) in 250 mL mili-Q water.

3.3.2 Preparation of 5 mM ferri/ferro cyanide redox couple

0.1646 g potassium ferricyanide ($K_3[Fe(CN_6)]$) and 0.2112 g potassium ferrocyanide ($K_4[Fe(CN_6)]$) were dissolved in 100 mL of 0.5 M KCl.

3.3.3 Preparation of 0.1 M hydrochloric acid solution

The dilute HCl solution was used as a supporting electrolyte for Pb^{2+} and Cd^{2+} determination. 0.1 M HCl solution was prepared by dilution of 2.08 mL HCl, fuming 37% to 250 mL of mili-Q water.

3.3.4 Preparation of stock standard solution of lead and cadmium

1 mg L^{-1} of mixed solution of Pb^{2+} and Cd^{2+} was prepared from 1000 mgL^{-1} standard solution by diluting 50 µL of Pb^{2+} and Cd^{2+} standard solution to 50 µL with 0.1 M HCl (pH 1.0).

3.3.5 Preparation of stock standard solution of bismuth

5 mg L^{-1} of bismuth (Bi^{+}) solution was prepared by diluting 250 µL of 1000 mg L^{-1} Bi^{3+} to 50 mL with 0.1 M HCl. The Bi^{3+} solution was used for in-situ plating of Bi^{3+}.

3.4 Optimization and modification of the electrode

3.4.1 Preparation of screen-printed carbon electrode

A carbon electrode was fabricated on a polyvinyl chloride (PVC) substrate using screen-printing technique. Initially, the silver/silver chloride (Ag/AgCl) ink was printed on PVC substrate as a conductive pad (Figure 3.1 step I). Then, the carbon ink was printed on top of patterned silver layer to be used as a working electrode area. The ink-coated PVC substrate was then dried in an oven at 55 ºC for 1 h after each screen-printing step to remove residual solvent (Figure 3.1 step II).

Step I. Ag/AgCl ink screen-printed

Step II. Carbon ink screen-printed

Front side Back side

Figure 3.1 Preparation of screen-printed carbon electrode using an in-house screen-printing technique.

3.4.2 Optimization of the modified electrode composition

3.4.2.1 Effect of type of carrier polymer

Carrier polymer was used to blend the conducting polymer (PANI) with nanocarbon material (G) to prepare electrospun nanoporousfiber. In this study, type of carrier polymer including polystyrene (PS), polycaprolactone (PCL), and poly(methyl methacrylate) (PMMA) were investigated. All carrier polymers were dissolved in THF at the same concentration as 23% w/v and using the same electrospinning condition. The electrochemical sensitivity of electrospun with different carrier polymers was studied by cyclic voltammetry using 1 mM of a standard $[Fe(CN)_6]^{3-/4-}$redox couple.

3.4.2.2 Effect of solvent system

The influence of solvent system on the morphology of G/PANI/PS electrospun fiber was investigated and optimized. A 23% w/v PS solution was prepared in different volumes of the THF/DMF (25/75 %, 50/50 %, 75/25 and THF 100 %). The morphologies of electrospun fiber with different solvent system were characterized by scanning electron microscope (SEM).

3.4.2.3 Effect of PS concentration

The effect of concentration of carrier polymer was investigated. The different concentration of PS as 10%, w/v, 13% w/v, 15% w/v 18% w/v, 20% w/v and 23 % w/v were dissolved in 100% THF and fabricated with the same condition of electrospinning process. The electrospun fiber morphologies obtained from different concentration were investigated by SEM.

3.4.2.4 Effect of G loading

Amount of G loading was investigated and optimized. The G nanopowders with 0, 2, 4, 6, 8, 10 mg were dispersed in 1 mL of DMF and sonication for 24 h. The influence of G loading was investigated by cyclic voltammetry using 1 mM of a standard $[Fe(CN)_6]^{3-/4-}$redox couple.

3.4.3 Electrospinning fabrication of screen-printed carbon electrode

3.4.3.1 Preparation of G/PANI/PS solution

The solution of G, PANI, and PS were prepared separately as follows. G nanopowders were dispersed in 1 mL of DMF and sonication for 24 h. For the PANI solution, PANI emeraldine base 0.60 g was doped with CSA 0.77 g and dissolve in 15 mL of $CHCl_3$. PANI solution was stirred at 1000 rpm for 6 h and filtered to obtain a clear PANI solution. 23% PS solution was prepared in 100 % of THF, PANI and G was mixed as ratio 1:1. After that, 150 µL of G/PANI, 1000 µL of 23% w/v PS solution were mixed together.

3.4.3.2 An electrospinning process

The mixture of G/PANI/PS was loaded into a syringe and fabricated onto screen-printed carbon electrode surface by electrospinning. An in-house electrospinning system was set up in horizontally for electrode modification, the voltage was 10.5 kV, the flow rate was 0.5 mL/h and needle tip-to collector distance was 15 cm. Finally, the fibers were collected on the screen-printed carbon electrode as shown in Figure 3.2.

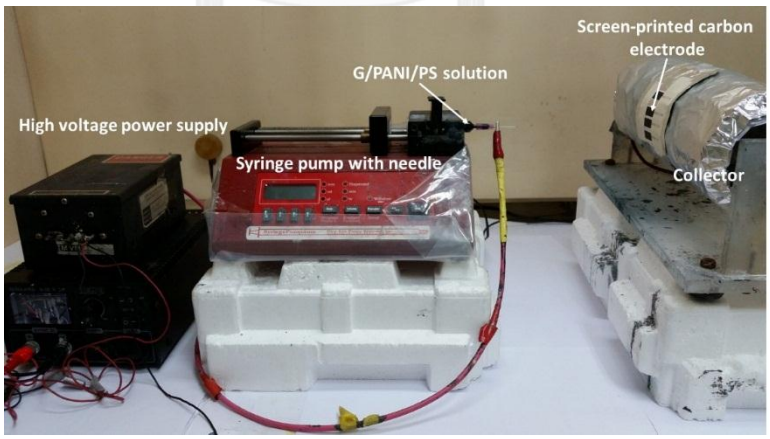

Figure 3.2 An in-house horizontally electrospinning set up used in this study.

3.4.4 Optimization of anodic stripping voltammetry

To obtain the high sensitivity of Pb^{2+} and Cd^{2+} determination, several parameters of anodic stripping voltammetry were investigated and optimized.

3.4.4.1 Effect of the type of supporting electrolyte

Type of supporting electrolyte is an important factor controlling the electrochemical sensitivity of the system. Thus, types of supporting electrolyte including hydrochloric acid, acetate buffer and phosphate buffer saline were investigated.

3.4.4.2 Effect of the bismuth concentration

In this study, in-situ of Bi^{3+} was used to increase sensitivity of electrochemical sensor for simultaneous determination of Pb^{2+} and Cd^{2+}. The effect of Bi^{3+} concentration with 100, 500, 900, 1300 and 1700 µg L^{-1} were investigated and optimized.

3.4.4.3 Effect of the square wave anodic stripping voltammetry parameters

The square wave anodic stripping voltammetry parameters including deposition potential, deposition time were investigated and optimized for the simultaneous detection of Pb^{2+} and Cd^{2+}. The deposition potential in the range -1.5 to -1.0 V, the deposition time in the range 60 to 300 s. The current response obtained from 200 µg Lof Pb^{2+} and Cd^{2+} in the presence of Bi^{3+} at each parameter.

3.5 Physical characterization

The morphology of electrospun nanoporous fibers on screen-printed carbon electrode (SPCE) surface was investigated using a JSM-6400 field emission scanning electron microscope and a transmission electron microscope. The surface area analysis of nanoporous fibers was performed using Brunauer–Emmett–Teller (BET) technique.

3.6 Electrochemical characterization

All electrochemical measurements were performed on a μAUTOLAB type III potentiostat controlled with General Purpose Electrochemical System (GPES) software. A three electrode system was used and consisted of an auxiliary Pt wire electrode, a reference Ag/AgCl electrode and the G/PANI/PS electrospun fibers modified SPCE as a working electrode. An in house electrochemical cell are showed in Figure 3.3.

Figure 3.3 An in-house electrochemical set up with 3 electrodes used in this study (WE: working electrode, CE: counter electrode, RE: reference electrode).

3.6.1 Cyclic voltammetry procedures

To study the behavior of the G/PANI electrospun fiber modified carbon electrode, 1.0 mM $[Fe(CN)_6]^{3-/4-}$ in 0.5 M KCl was used with the scanning potential from -0.5 to +1 V at a scan rate of 100 mV S^{-1}.

3.6.2 Square wave anodic stripping voltammetry procedures

For the simultaneous determination of Pb^{2+} and Cd^{2+}, the square wave anodic stripping voltammetry (SWASV) was employed under optimal conditions with in-situ of Bi^{3+}. The optimal condition includes a deposition potential of -1.2 V, a deposition time of 180 s, a frequency of 100 Hz, a potential amplitude of 40 mV, and a step potential of 21 mV.

3.7 The analytical performance of G/PANI/PS porous fiber modified carbon electrodes

3.7.1 Calibration curve and liner range

The different concentration of mixed Pb^{2+} and Cd^{2+} standard solution were measured on G/PANI/PS nanoporous electrospun fiber modified carbon electrode. The calibration curve and linearity were obtained from the linear plot of concentration versus current response.

3.7.2 Limit of detection

The limit of detection (LOD) was calculated by LOD = $3S_b/m$, where S_b is a standard deviation of the blank (estimated by 8 replicatesof the blank signals), m is a slope of calibration graph [35].

3.7.3 Limit of quantitation

The limit of detection (LOQ) was calculated by LOD = $10S_b/m$, where S_b is a standard deviation of the blank (estimated by 8 replicates of the blank signals), m is a slope of calibration graph [35].

3.7.4 Repeatability

The repeatability of modified electrode was investigated by measuring ten replicates of 200 μg L^{-1} Pb^{2+} and Cd^{2+}. The percentage of relative standard deviation (%RSD) was calculated by

$$\%RSD = \frac{\text{standard deviation}}{\text{mean}} \times 100$$

3.7.5 Recovery

The recovery was used to validate proposed system compare with the conventional method as inductively coupled plasma optical emission spectroscopy (ICP-OES). The recovery was calculated by

$$\%\text{Recovery} = \frac{\text{measured value of the spiked sample-measured value of the unspiked sample}}{\text{known value of the spike in the sample}} \times 100$$

3.7.6 Interference study

For the interference study of G/PANI/PS nanoporous electrospun modified carbon electrode, the effect of commonly species in the river water such as Na^{+}, K^{+}, Mg^{2+}, Ca^{2+},Fe^{3+}, Co^{2+}, Ca^{2+}, Ba^{2+}, Ni^{2+}, Cu^{2+} ,Zn^{2+},Cl^{-}, SO_4^{2-} and NO_3^{-} were evaluated at 50 μg L^{-1} of Pb^{2+} and Cd^{2+}. The tolerance ratio is defined as the peak response change ± 5% from the Pb^{2+} and Cd^{2+} anodic peaks in the presence of these foreign ions.

3.8 Real sample analysis

3.8.1 Preparation of river water samples

The river water samples were collected from different river sources (*i.e.* Chao Phraya river, Saen Saeb canal). Firstly, the all river water samples were spike with known amount of Cd^{2+} and Pb^{2+}. Then, river water samples were heated to boil on a hot plate. Two aliquots of milli Q water were added to the samples. Between each addition of milli Q water, the sample solution was allowed to evaporate by heating to eliminate the residue of nitric acid [61]. Lastly, the pH and final volume of digested solution was then adjusted with supporting electrolyte of 0.1 M HCl (pH 1.0) and then stored in a freezer. The recovery and precision of the acid digestion method were evaluated by using standard addition method [2, 61] for the analysis of water samples following spiking with either metal ions at final concentrations of 25, 50 and 150 μg L^{-1}. For method validation, the results obtained from the proposed system were compared with those obtained from ICP-OES technique.

CHAPTER IV
RESULTS AND DISCUSSION

This chapter, the results of G/PANI/PS nanoporous fiber modified screen-printed carbon electrode will be discussed. These results include the optimization of electrode modification, the characterization of electrode morphology, the electrochemical characterization of modified electrode, the analytical performances of modified electrode, the optimization of anodic stripping voltammetry, interference study and the real sample analysis.

4.1 Optimization of the electrode modification

The parameters affecting the fiber morphology and electrochemical sensitivity of electrospun G/PANI/PS nanoporous fibers modified carbon electrode, such as type of carrier polymer, type of organic solvent used for carrier polymer dissolution, concentration of carrier polymer and amount of G loading were investigated and optimized.

4.1.1 Type of carrier polymer

Three polymers (polystyrene (PS), polycaprolactone (PCL) and poly (methyl methacrylate) (PMMA)) were chosen as a possible carrier based on the compatibility with PANI, dissolution ability with PANI common solvent, processability, and availability. Figure 4.1, showed SEM images of PS, PCL and PMMA electrospun fibers under the same processing condition, *i.e*. 20% by wt polymer concentration, 10.5 kV, 15 cm gap distance and 0.5 mL/hr flow rate. The PS and PMMA fiber were slightly collapsed along fiber axis with surface pores appeared throughout, while PCL fibers looked whole with smooth surface. The average size of PS, PCL and PMMA fibers was 2.44±0.53 μm, 0.31±0.1 μm and 3.28±0.87μm, respectively.

The effect of carrier polymer type on the electrochemical sensitivity of G/PANI fiber modified carbon electrode was investigated by cyclic voltammetry using a standard $[Fe(CN)_6]^{3-/4-}$ redox couple. Surprisingly, as shown in Figure 4.2, the anodic peak current response measured on the electrospun G/PANI with PS as carrier polymer

is higher than both PCL and PMMA, despite the fact that PS fibers size was the largest. Since fibers with smaller size would have a higher surface area and help increase sensor performance, the result indicated that other factors, such as fiber arrangement, fiber density or the way that G/PANI distribute in carrier polymer, might have come into play. Based on processability, relatively ease of porous surface manipulation and, most importantly sensor sensitivity, PS was chosen as a carrier polymer for the further studies.

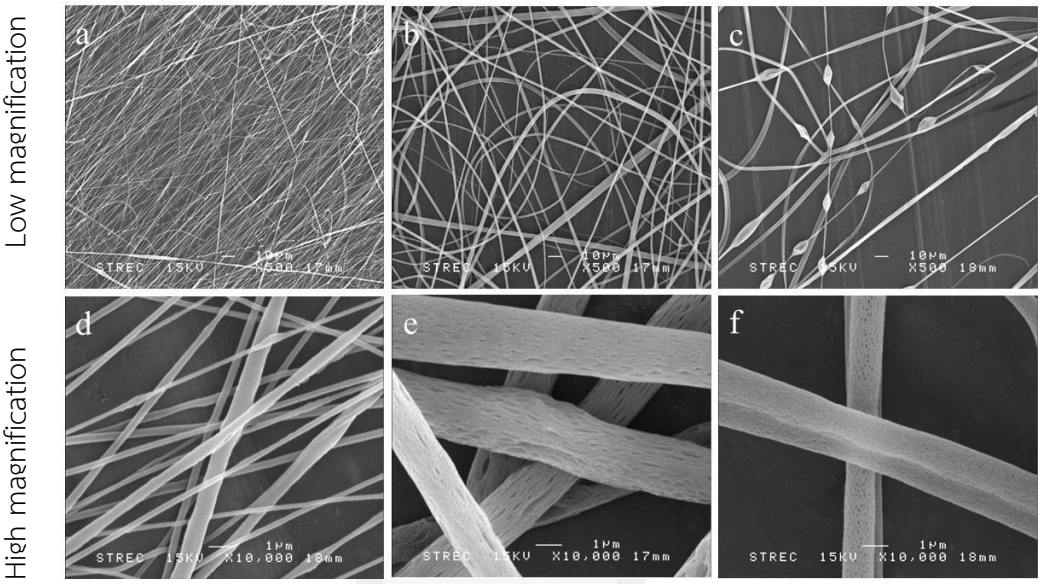

Figure 4.1 SEM images of electrospun fibers from different carrier polymer. (a,d) PCL, (b,e) PS, (c,f) PMMA.

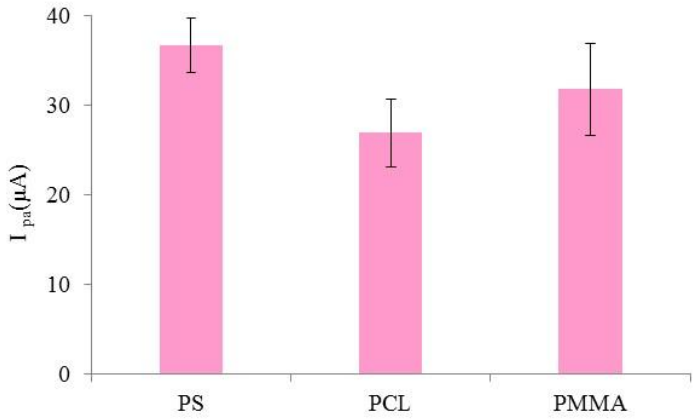

Figure 4.2 Anodic peak current (I_{pa}) obtained from the cyclic voltammetry of 1.0 mM $[Fe(CN)_6]^{3-/4-}$ in 0.5 M KCl using G/PANI nanoporous fiber modified carbon electrodes with different type of carrier polymer. The error bars correspond to the standard deviation obtained from 3 measurements (n=3).

4.1.2 Effect of solvent system

The morphologies of electrospun G/PANI/PS fibers produced from different solvent system were investigated by SEM as showed Figure 4.3. The formation of small ridges of G/PANI/PS fibers is observed and they increase when the percentage of THF increases from 25% to 100% (Figure 4.3a to 4.3d) and the highest of THF (Figure 4.3d), the nanopores was observed on the elestrospun fibers surface. This suggests that the porous on the electrospun G/PANI/PS fibers was generated by the different evaporation rate of THF (boiling point of 66 °C) and DMF (boiling point of 153 °C) and moisture effect leading to microphase separation on fiber surface before the solidification. The nanoporous electrospun G/PANI fibers prepared from 100%THF provide the highest surface area compared to other solvent systems. Therefore, 100% THF was chosen for subsequent studies.

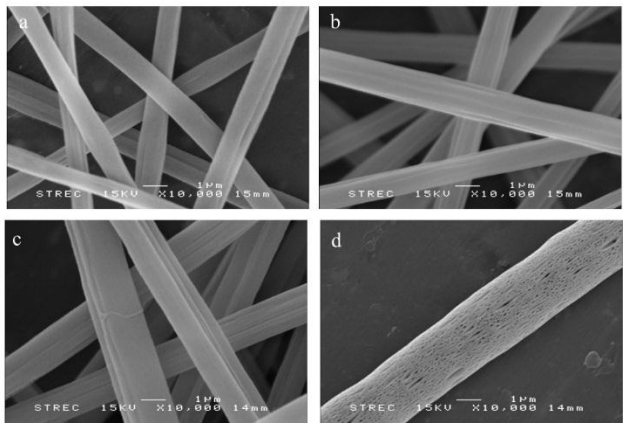

Figure 4.3 SEM images of electrospun fibers obtained from different solvent systems (a) 25/75% THF/DMF, (b) 50/50% THF/DMF, (c) 75/25% THF/DMF, (d) 100% THF.

4.1.3 Effect of PS concentration

The influence of carrier polymer concentration on G/PANI/PS nanoporous fiber mophology was investigated. When the concentration of PS increased, the diameter and roughness of fiber surface increased (Figure 4.4). At the 20% w/v of PS, the electrospun G/PANI was generated continuously with the uniform nanopores on the electrospun fiber surface, thus, 20% w/v of PS was selected for this experiment.

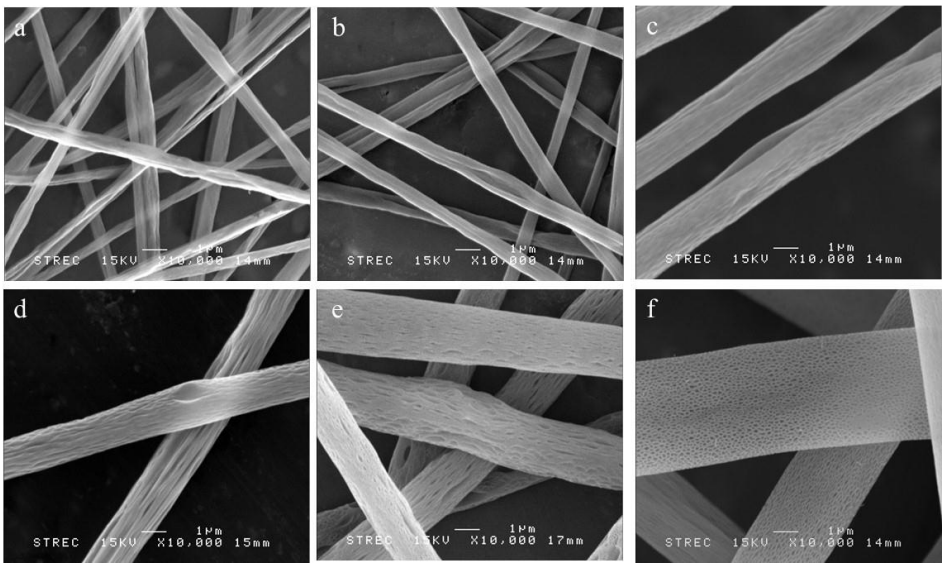

Figure 4.4 SEM images of electrospun fibers obtained from different concentrations of PS (a) 10% w/v PS, (b) 13% w/v PS, (c) 15% w/v PS, (d) 18% w/v PS, (e) 20% w/v PS, (f) 23% w/v PS.

4.1.4 Effect of G loading

To optimize the amount of G loading on G/PANI/PS nanoporous fiber modified electrodes, cyclic voltammetry using a standard $[Fe(CN)_6]^{3-/4-}$ redox couple was performed. Figure 4.5 shows the anodic peak current response measured on the G/PANI/PS nanoporous fibers modified electrode with different amount of G loading from 0 to 10 mg/mL. The anodic current responses increase from 0 mg/mL to 4 mg/mL of G and the anodic peak currents decrease afterwards. This is probably caused by the self-agglomeration of G inside the nanoporous fiber, leading to decreased surface area and electrochemical conductivity. Therefore, 4 mg/mL of G loading was chosen for further experiments.

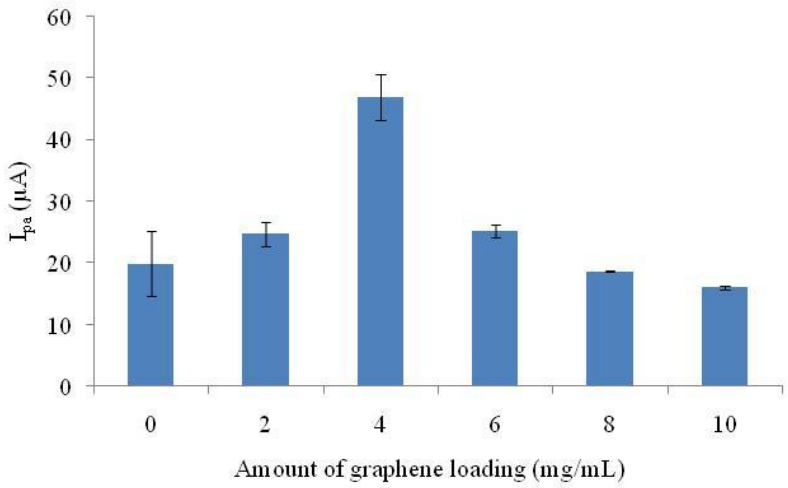

Figure 4.5 Anodic peak current (I_{pa}) obtained from the cyclic voltammetry of 1.0 mM $[Fe(CN)_6]^{3-/4-}$ in 0.5 M KCl using G/PANI/PS nanoporous fiber modified carbon electrodes with different amount of G loading. The error bars correspond to the standard deviation obtained from 5measurements (n=5).

Among all the factors, type of organic solvent and percentage of G loading are the two significant factors controlling the morphology and electrochemical sensitivity of G/PANI/PS nanoporous fiber modified carbon electrode.

4.2 Electrode morphology characterization

The morphology of the G/PANI/PS nanoporous fibers was characterized by scanning electron microscope (SEM) and transmission microscope (TEM). As shown in Figure 4.6a and 4.6b, the nanoporous fibers with an average diameter of 2.44±0.53 μm were created on the modified carbon electrode surface and the nanoporous structures with size in the range of 100-200 nm was found on the electrospun fibers. The TEM image of nanoporous fibers (Figure 4.6c) verifies that G is randomly distributed inside the fiber with no agglomerations within the nanoporous fibers. The brightness of the TEM image is related to electron density of atom or the specimen thickness, the bright are void or open cavities in the matrix. The BET technique was used to measure the surface area of nanoporous fibers and it was found to be 12.23 m^2/g, which is relative high for electrospun fiber of this size range.

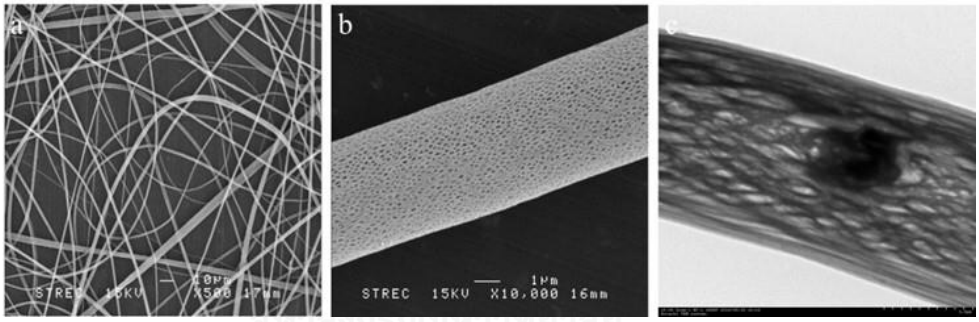

Figure 4.6 SEM images of the G/PANI/PS nanoporous fibers (a) low magnification, (b) high magnification and (c) TEM image of random distribution of G in the G/PANI/PS nanoporous fibers.

4.3 The electrochemical characterization

Cyclic voltammetry (CV) using 1.0 mM $[Fe(CN)_6]^{3-/4-}$ as a redox couple was used to characterize the electrochemical characteristics of unmodified carbon electrode, PANI/PS nanoporous fiber modified carbon electrode and G/PANI/PS nanoporous fiber modified carbon electrode (Figure 4.7). The current response of G/PANI/PS nanoporous fiber modified carbon electrodes is higher than unmodified carbon electrode and PANI/PS modified carbon electrodes approximately 3 times and 2 times, respectively.

The significant increase of current response indicates the enhanced electrochemical sensitivity of G/PANI/PS nanoporous fiber modified carbon electrode.

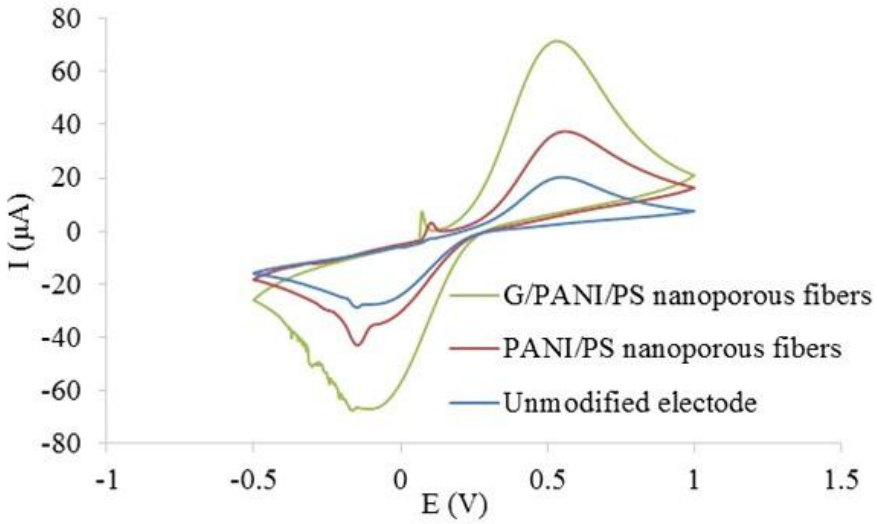

Figure 4.7 Cyclic voltammograms of 1.0 mM $[Fe(CN)_6]^{3-/4-}$ in 0.5 M KCl using the unmodified carbon electrode, PANI/PS nanoporous fiber modified carbon electrode and G/PANI/PS nanoporous fiber modified carbon electrode.

4.4 The performance of the G/PANI/PS nanoporous fiber modified carbon electrodes

To evaluate the electrochemical behavior of G/PANI/PS nanoporous fiber modified carbon electrodes, the reversible electron transfer of $[Fe(CN)_6]^{3-/4-}$ in the different scan rates was investigated on this electrode and the data conformed to Randles-Sevcik equation (Figure 4.8). As expected the anodic and cathodic peak currents increase with the scan rate (Figure 4.9). The linearity of anodic and cathodic peak currents versus the square root of the scan rate in the range from 10-100 mV s^{-1} indicated that the redox reaction occurred on this electrode is diffusion controlled process.

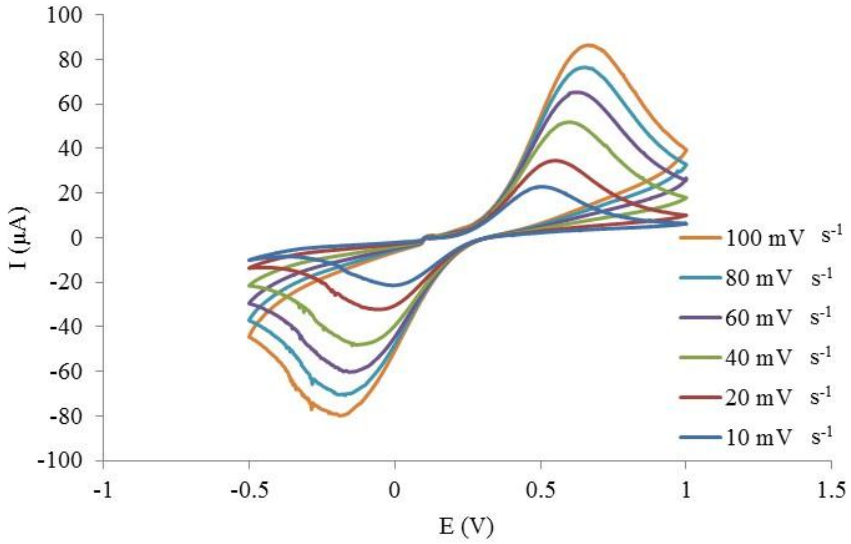

Figure 4.8 Cyclic voltammograms of 1.0 mM $[Fe(CN)_6]^{3-/4-}$ in 0.5 M KCl using the G/PANI/PS nanoporous fiber modified carbon electrode at scan rate of 10, 20,40,60,80,100 mV s^{-1}.

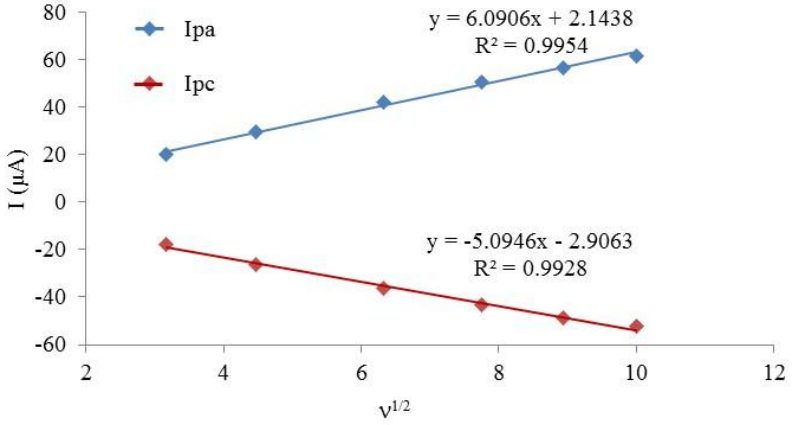

Figure 4.9 The anodic (I_{pa}) and cathodic (I_{pc}) peak currents of 1.0 mM $[Fe(CN)_6]^{3-/4-}$ in 0.5 M KCl as a function of the square root scan rate, measure on the G/PANI/PS nanoporous fiber modified carbon electrode.

4.5 The optimization of square wave anodic stripping voltammetry

The G/PANI/PS nanoporous fiber modified carbon electrode was applied for the simultaneous detection of Pb^{2+} and Cd^{2+} by using square wave anodic stripping voltammetry (SWASV). To obtain the high sensitivity for the simultaneous determination of Pb^{2+} and Cd^{2+}, several parameters affecting the current response of the G/PANI/PS nanoporous fiber modified carbon electrodes, such as supporting electrolyte, concentration of Bi^{3+}, deposition potential, deposition times were optimized. In this study, 100 Hz of frequency, 40 mV of potential amplitude, 21 mV of step potential were selected as the experimental conditions for SWASV measurement.

4.5.1 Effect of the supporting electrolyte

The influence of supporting electrolytes in the detection of Pb^{2+} and Cd^{2+} in the presence of Bi^{3+} on G/PANI/PS nanoporous fibers was investigated by using supporting electrolytes (0.1 M HCl, 0.1 M NaAc/HAc, 0.1 M PBS). Figure 4.10 and Figure 4.11 show the anodic voltammograms and the stripping peak current of 200 μg L^{-1} Pb^{2+} and Cd^{2+} in presence of 500 μg L^{-1} Bi^{3+} with different supporting electrolytes measured on G/PANI/PS nanoporous fiber modified electrode. As shown in Figure 4.11, the highest stripping peak currents of both Pb^{2+} and Cd^{2+} was obtained when 0.1 M HCl (pH 1.0) was used as a supporting electrolyte. Thus, 0.1 M HCl (pH 1.0) was chosen as a supporting electrolyte for the further experiments.

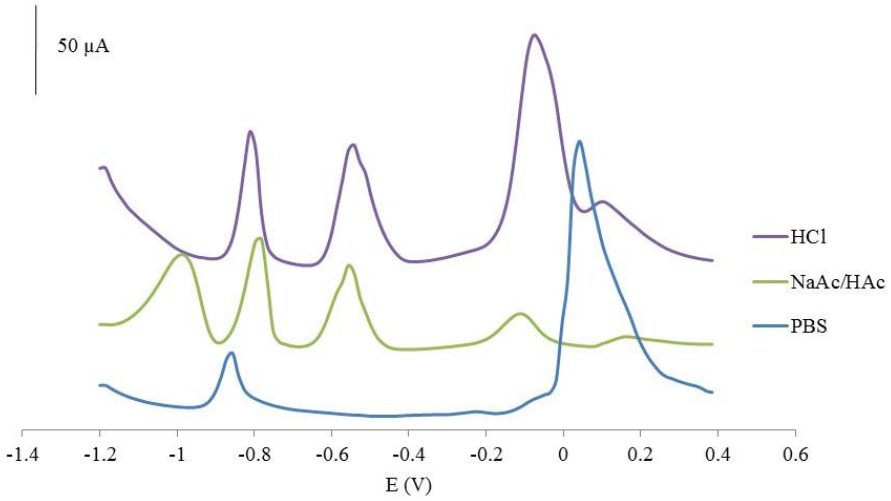

Figure 4.10. Anodic stripping voltammograms of 200 µg L^{-1} Pb^{2+} and Cd^{2+} with 500 µg L^{-1} Bi^{3+} in 0.1 M PBS (pH 7.0), 0.1 M NaAc/HAc (pH 4.5), and 0.1 M HCl (pH 1.0) as the supporting electrolytes using the G/PANI/PS nanoporous fiber modified carbon electrode. Measurement parameters: deposition potential of -1.2 V, deposition times of 120 s, frequency of 35 Hz, potential amplitude of 15 mV, and step potential of 100 mV.

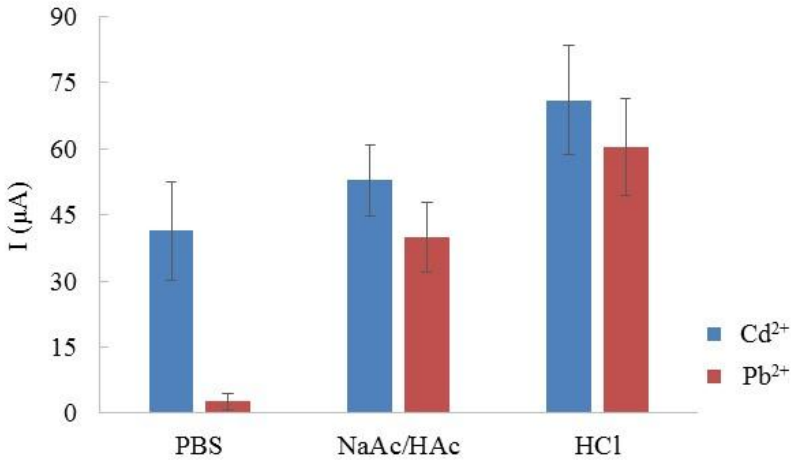

Figure 4.11 The stripping peak current of 200 µg L^{-1} Pb^{2+} and Cd^{2+} with 500 µg L^{-1} Bi^{3+} in 0.1 M PBS (pH 7.0), 0.1 M NaAc/HAc (pH 4.5), and 0.1 M HCl (pH 1.0) using the G/PANI/PS nanoporous fiber modified carbon electrode. Measurement parameters are same in the Figure 4.10. The error bars correspond to the standard deviation obtained from 3 measurements (n=3).

4.5.2 Effect of the bismuth concentration

The influence of Bi^{3+}concentration on the simultaneous determination of Pb^{2+} and Cd^{2+} was investigated and optimized in a range of 100 – 1700 μg L^{-1}. Figure 4.12 shows the anodic striping voltammograms of Pb^{2+} and Cd^{2+} with different concentrations of Bi^{3+} measured on the G/PANI/PS nanoporous fiber modified electrodes. As show in Figure 4.13, the peak current of Cd^{2+} rapidly increases when the concentration of Bi^{3+} increases from 100 to 900 μg L^{-1} and the peak current of Pb^{2+} slowly increases over the range 100 to 900 μg L^{-1}. At high concentrations of Bi^{3+} solution, the stripping peak responses of Cd^{2+} and Pb^{2+} decrease, which probably because of the mass transfer limitation of Cd^{2+} and Pb^{2+} diffusing out from the Bi-thick film during the stripping step. Therefore, 900 μg L^{-1} of Bi^{3+} was selected for the subsequent measurements.

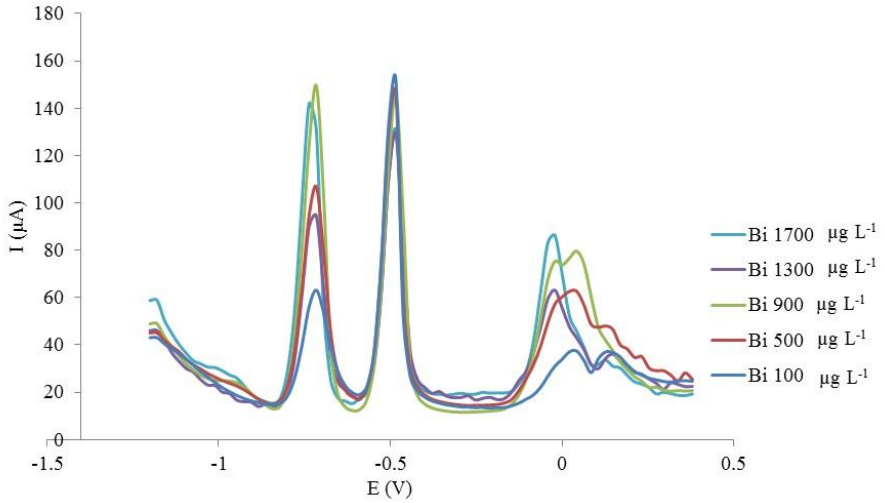

Figure 4.12 Anodic stripping voltammograms of 200 μg L^{-1} Pb^{2+} and Cd^{2+} in 0.1 M HCl (pH 1.0) with different concentration of Bi^{3+} measured on the G/PANI/PS nanoporous fiber modified carbon electrode. Measurement parameters: deposition potential of -1.2 V, deposition times of 120 s, frequency of 100 Hz, potential amplitude of 40 mV, and step potential of 21 mV.

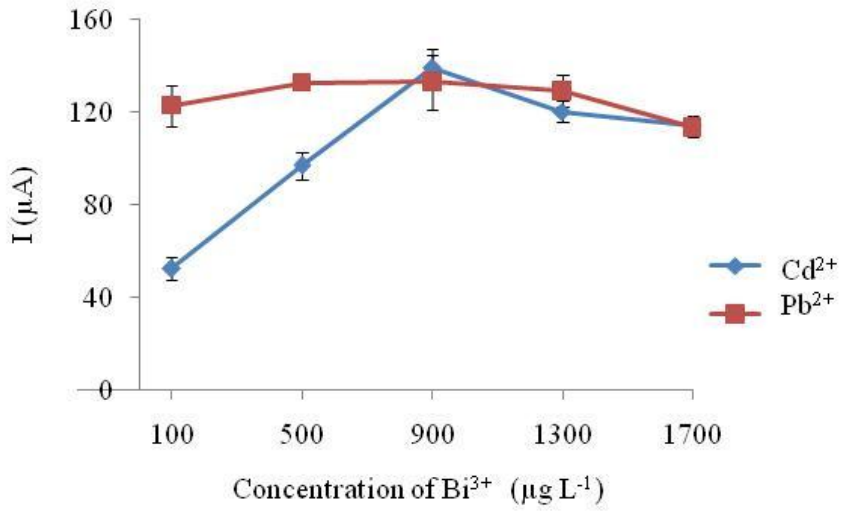

Figure 4.13 Effect of Bi^{3+} concentration on the peak currents of 200 µg L^{-1} Pb^{2+} and Cd^{2+} in 0.1 M HCl (pH 1.0). Measurement parameters are same in the Figure 4.12. The error bars correspond to the standard deviation obtained from 5 measurements (n=5).

4.5.3 Effect of the deposition potential

The effect of the deposition potential of Pb^{2+} and Cd^{2+} on the G/PANI/PS nanoporous fiber modified electrodes was investigated in a range from -1.5 to -1.0 V. The anodic striping voltammograms at different deposition potential of 200 µg L^{-1} Pb^{2+} and Cd^{2+} in the presence of 900 µg L^{-1} of Bi^{3+} in 0.1 M HCl (pH 1.0) are shown in Figure 4.14. The current response of the anodic stripping voltammogram Pb^{2+} and Cd^{2+} increases from -1.0 to -1.2 V and the deposition potential more negative than -1.2 V, the current response decreased because of hydrogen evolution. The highest peak current of both Pb^{2+} and Cd^{2+} were obtained at -1.2 V (Figure 4.15). Thus, deposition potential at -1.2 V was chosen for the measurement.

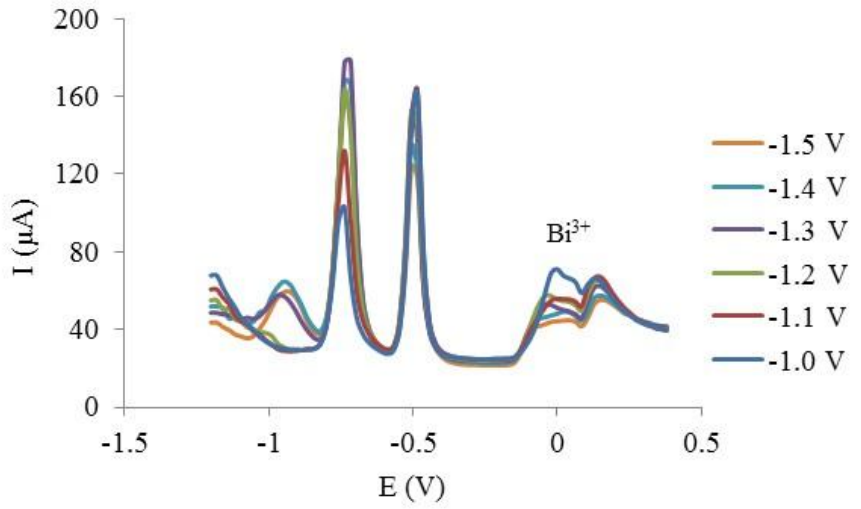

Figure 4.14 Anodic stripping voltammograms of 200 μg L^{-1} Pb^{2+} and Cd^{2+} with 900 μg L^{-1} Bi^{3+} in 0.1 M HCl (pH 1.0) at the different deposition potential measured on the G/PANI/PS nanoporous fiber modified carbon electrode. Measurement parameters: deposition times of 120 s, frequency of 100 Hz, potential amplitude of 40 mV, and step potential of 21 mV.

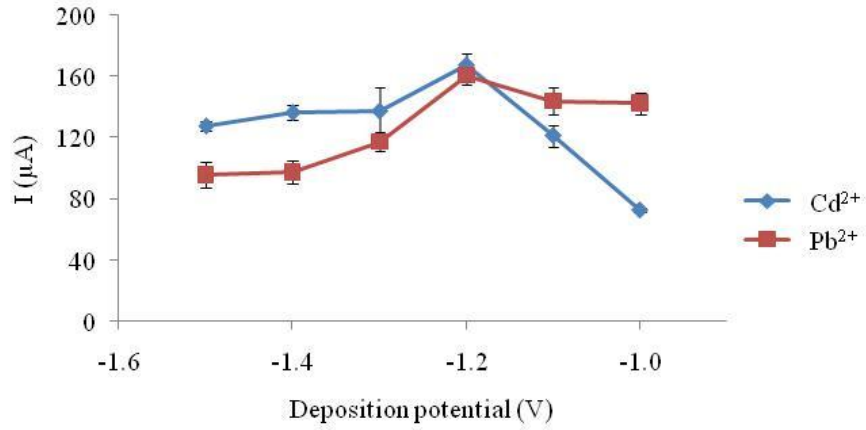

Figure 4.15 Effect of deposition potential on the peak currents of 200 μg L^{-1} Pb^{2+} and Cd^{2+} with 900 μg L^{-1} Bi^{3+} in 0.1 M HCl (pH 1.0). Measurement parameters are same in the Figure 4.14. The error bars correspond to the standard deviation obtained from 5 measurements (n=5).

4.5.4 Effect of the deposition time

The effect of the deposition time on the current response of Pb^{2+} and Cd^{2+} on G/PANI/PS nanoporous fiber modified electrodes was studied in a range from 60 to 300 s. Figure 4.16 shows the anodic striping voltammograms of Pb^{2+} and Cd^{2+} with different deposition time measured on the G/PANI/PS nanoporous fiber modified electrodes. The results show in Figure 4.17, the peak current of both Pb^{2+} and Cd^{2+} rapidly increased from 60 to 180 s and slowly decreased after 180 s. This is probably due to the electrode fouling from the excess amount of deposition metals on the electrode surface. Therefore, 180 s of deposition times was chosen for the further measurements.

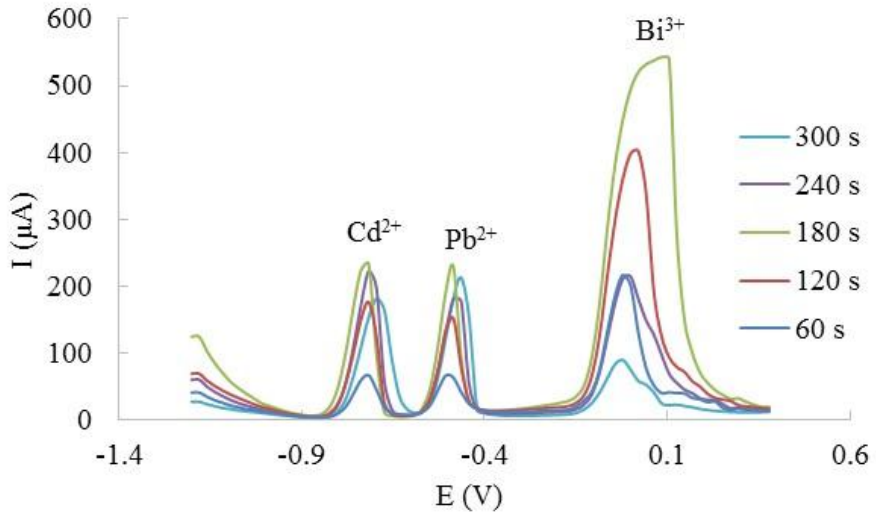

Figure 4.16 Anodic stripping voltammograms of 200 µg L^{-1} Pb^{2+} and Cd^{2+} with 900 µg L^{-1} Bi^{3+} in 0.1 M HCl (pH 1.0) at the different deposition time measured on the G/PANI/PS nanoporous fiber modified carbon electrode. Measurement parameters: deposition potential of -1.2 V, frequency of 100 Hz, potential amplitude of 40 mV, and step potential of 21 mV.

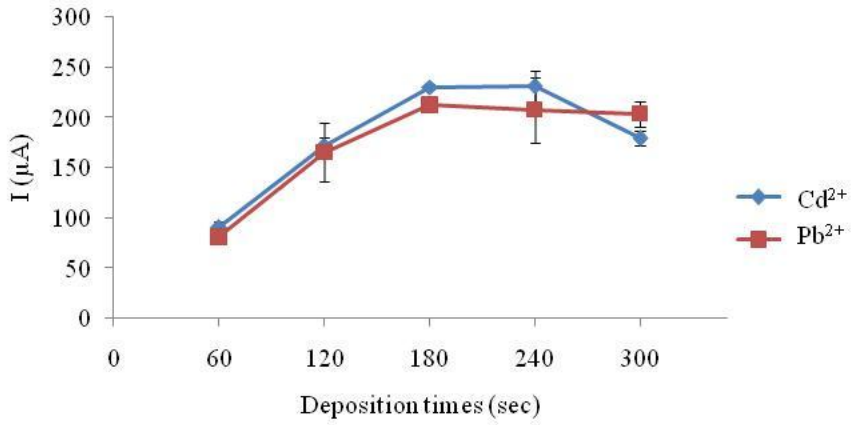

Figure 4.17 Effect of deposition times on the peak currents of 200 µg L^{-1} Pb^{2+} and Cd^{2+} with 900 µg L^{-1} Bi^{3+} in 0.1 M HCl (pH 1.0). Measurement parameters are same in the Figure 4.16. The error bars correspond to the standard deviation obtained from 5 measurements (n=5).

4.6 Analytical performance of the G/PANI/PS nanoporous fiber modified carbon electrodes

The electrode performances were studied, under the optimum conditions using different electrodes. The optimum conditions include: HCl solution as supporting electrolyte (pH 1.0); Bi^{3+} concentration 900 µg L^{-1}; deposition potential -1.2 V; deposition potential 180 s; frequency 100 Hz; potential amplitude 40 mV; step potential 21 mV and using 200 µg L^{-1} Pb^{2+} and Cd^{2+}. Three different electrodes are unmodified carbon electrode, PANI/PS nanoporous fiber modified electrode and G/PANI/PS nanoporous fiber modified carbon electrode are shown in Figure 4.18. The peak current of G/PANI/PS nanoporous fiber modified electrodes was higher than unmodified electrode and PANI/PS nanoporous modified electrodes approximately 8 times and 3 times for Cd^{2+} detection and peak current of Pb^{2+} detection of G/PANI/PS nanoporous fiber modified carbon electrodes was higher than unmodified carbon electrode and PANI/PS nanoporous fiber modified carbon electrodes approximately 5 times and 2 times, respectively. Comparing to the absence of Bi^{3+}, the presence of Bi^{3+} also improves the electrochemical sensitivity of this sensor in the simultaneous detection of Pb^{2+} and Cd^{2+}.

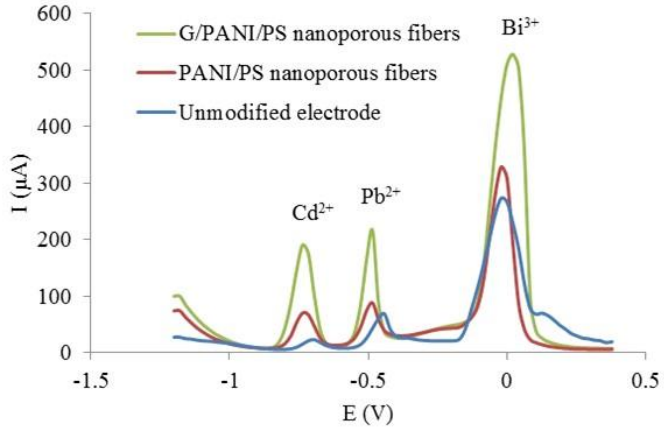

Figure 4.18 Anodic stripping voltammograms of 200 μg L^{-1} Pb^{2+} and Cd^{2+} with 900 μg L^{-1} Bi^{3+} in 0.1 M HCl (pH 1.0). Measurement parameters: -1.2 V deposition potential, 180 s deposition potential, 100 Hz frequency, 40 mV potential amplitude, and 21 mV step potential using the unmodified carbon electrode, PANI/PS nanoporous fiber modified carbon electrode and G/PANI/PS nanoporous fiber modified carbon electrode.

The analytical performances of G/PANI/PS nanoporous fiber modified carbon electrodes for the simultaneous determination of Pb^{2+} and Cd^{2+} with under the optimal conditions were evaluated. The anodic stripping voltammograms of different concentration of Pb^{2+} and Cd^{2+} and the linear range in 10-500 μg L^{-1} with a correlation coefficient (R^2) of 0.9921 for Pb^{2+} and 0.9913 for Cd^{2+} are shown in figure 4.19 and 4.20a-4.20b. The limits of detection (LOD) calculated by LOD = $3S_b/m$, and the limit of quantitation (LOQ) calculated by, LOQ = $10S_b/m$ where S_b is a standard deviation of the blank (estimated by 8 replicate determination of the blank signals), m is a slope of calibration graph [35]. The limit of detection (LOD) was found to be 3.30 μg L^{-1} for Pb^{2+} and 4.43 μg L^{-1} for Cd^{2+} and the limit of quantitation (LOQ) was found to be 11.02 μg L^{-1} for Pb^{2+} and 14.78 μg L^{-1} for Cd^{2+}. However, the National Environment Board has considered maximum level 50 μg L^{-1} of Pb^{2+}, 50 μg L^{-1} of Cd^{2+} (when water hardness more than 100 mg L^{-1} as $CaCO_3$) and 5 μg L^{-1} of Cd^{2+} (when water hardness not more than 100 mg L^{-1} as $CaCO_3$) [80] in river water, the proposed system is acceptable and it might be alternative tool for Pb^{2+} and Cd^{2+} determination in the real river water samples.

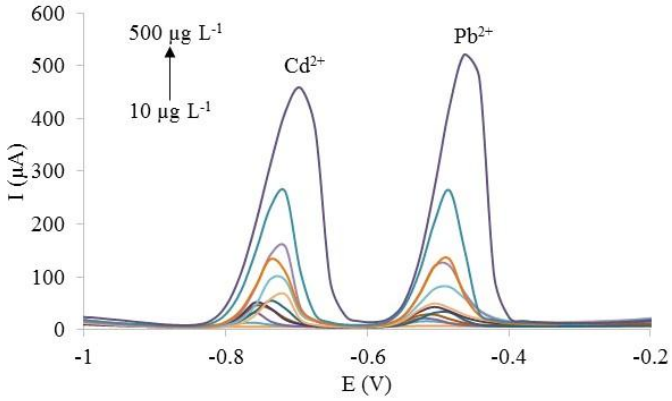

Figure 4.19 Anodic stripping voltammograms of Pb^{2+} and Cd^{2+} in the concentration range of 10-500 µg L^{-1} in the same conditions as Figure 4.18.

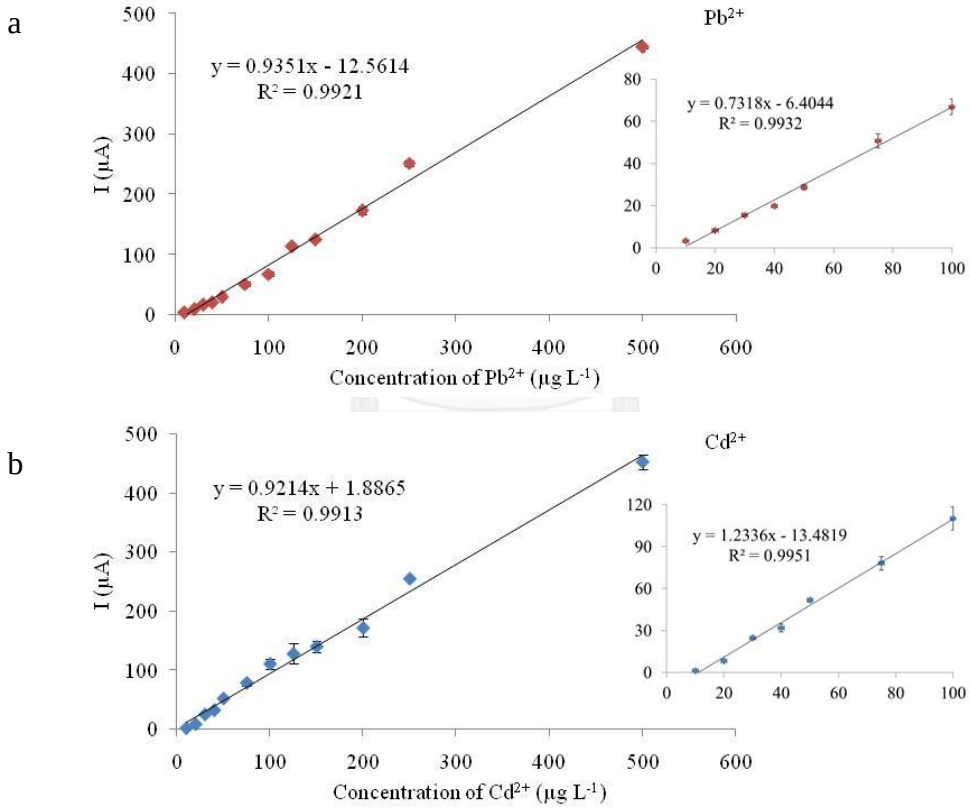

Figure 4.20 The linear plot of Pb^{2+} concentration versus the current response (inset: linear plot of the concentration of 10-100 µg L^{-1}) (a) and linear plot of Cd^{2+} concentration versus the current response (inset: linear plot of the concentration of 10-100 µg L^{-1}) (b). The error bars correspond to the standard deviation obtained from 5 measurements (n=5).

4.7 Reproducibility and stability of the modified electrode

The reproducibility and stability of G/PANI/PS nanoporous fiber modified carbon electrode were investigated by measuring the current response of 200 μg L^{-1} Pb^{2+} and Cd^{2+} with 900 μg L^{-1} Bi^{3+} in 0.1 M HCl (pH 1.0). The reproducibility of modified electrode was obtained from five different electrodes fabricated same condition, the relative standard deviation (RSD) was found to be 3.88% for Pb^{2+} and 3.55% for Cd^{2+}. The stability of this system was measured ten times in the same condition, and the RSD was found to be 4.67% for Pb^{2+} and 3.52% for Cd^{2+}.

Table 4.1 shows the comparison of G/PANI/PS nanoporous fiber modified carbon electrode with different electrodes in the previous reports for Pb^{2+} and Cd^{2+}determination. The proposed system provides a comparable detection limit and wide linear range for the simultaneous determination of Pb^{2+} and Cd^{2+}.

Table 4.1 Comparison of proposed electrode to different modified electrode for determination of Pb^{2+} and Cd^{2+}.

Electrode	Detection limit (μg L^{-1})		Linear range (μg L^{-1})		Ref
	Pb^{2+}	Cd^{2+}	Pb^{2+}	Cd^{2+}	
MWCNTs/ Schiff base /CPE	0.25	0.74	0.4 - 1100	1 – 1200	[35]
Bi film/ crown ether/ Nafion /SPCE	0.11	0.27	0.5-60	0.5-60	[45]
TiO_2/ZrO_2 composite /CPE	0.48	0.77	1 - 200	1 – 200	[81]
ERGNO film/SPCE	0.80	0.50	1 - 60	1 – 60	[82]
Bi-CNT/SPCE	1.3	0.7	2-100	2-100	[83]
P(DPA-co-2ABN)/GC	165	255	260-58730	1260-907800	[84]
Diacetyldioxime/CPE	2.07	4.48	20.7-3105	28-2800	[85]
PANI/ GC	20.7	14.56	0 - 414	0 - 224	[18]
G/PANI nanoporous fiber/SPCE	3.30	4.43	10-500	10-500	This work

MWCNTs; multi-walled carbon nanotubes, CPE; carbon paste electrode, SPCE; screen-printed carbon electrode, TiO2; titanium dioxide, ZrO2; zirconium dioxide, ERGNO; electrochemically reduced graphene oxide, Bi; bismuth, GC; glassy carbon electrode, CNT; carbon nanotube, P(DPA-co-2ABN); Poly(diphenylamine-co-2-aminobenzonitrile).

4.8 Interference study

In river water samples, there are many other ions interfering Pb^{2+} and Cd^{2+} detection. Thus, the influence of other cations and anions on the simultaneous determination of 50 μg L^{-1} Pb^{2+} and Cd^{2+} were investigated. The results show that a 500-flod mass ratio of Na^{+}, K^{+}, Mg^{2+}, ,Fe^{3+}, Co^{2+}, Cl^{-} and SO_4^{2-},a 250-fold mass ratio of Ca^{2+}, $Ba^{2+}$and NO_3^{2-},a 20-fold mass ratio of Ni^{2+} and a 1-fold mass ratio of Cu^{2+} and Zn^{2+} were not interfere of Pb^{2+} and Cd^{2+} determination. However, Cu^{2+} and Zn^{2+} were interfered more than other ions. This is probably cause by competition between Bi^{3+} and Cu^{2+}on the surface electrode and intermetallic compound phenomena [44, 86].

4.9 Real samples analysis

The proposed system was applied for environmental monitoring, the G/PANI/PS nanoporous fiber modified carbon electrode was used to measure Pb^{2+} Cd^{2+} in river water samples. The results obtained from our system were compared with the conventional method as ICP-OES method (table 4.2 and table 4.3). The %recoveries were found in the range of 85-109 % for Pb^{2+} and 95-103 % for Cd^{2+}.

Table 4.2 Determination of Pb^{2+} in various water samples using the proposed electrodes along with SWASV and ICP-OES method. The error bars correspond to the standard deviation obtained from 5 measurements (n=5).

Sample	Added ($\mu g\ L^{-1}$)	Pb^{2+}		Recovery (%)
	Pb^{2+}	ICP-OES ± SD ($\mu g\ L^{-1}$)	Found ± SD ($\mu g\ L^{-1}$)	Pb^{2+}
Chao Phraya river	0	15.05±0.62	10.30±0.47	-
	25	38.60±0.63	32.94±2.64	89.93±11.02
	50	61.12±0.25	53.02±2.05	85.43±4.11
	150	165.14±0.36	155.68±8.01	96.92±5.43
Saen Saeb canal	0	14.09±0.98	11.07±0.40	-
	25	42.69±0.51	38.11±1.05	107.79±4.21
	50	62.58±2.06	65.94±3.30	109.54±6.61
	150	168.97±0.49	159.08±0.90	98.61±0.60

Table 4.3 Determination of Cd^{2+} in various water samples using the proposed electrodes along with SWASV and ICP-OES method. The error bars correspond to the standard deviation obtained from 5 measurements (n=5).

Sample	Added ($\mu g\ L^{-1}$)	Cd^{2+}		Recovery (%)
	Cd^{2+}	ICP-OES ± SD ($\mu g\ L^{-1}$)	Found ± SD ($\mu g\ L^{-1}$)	Cd^{2+}
Chao Phraya river	0	3.18±0.07	ND	-
	25	24.86±0.05	24.92±2.40	98.68±9.61
	50	46.65±0.04	51.84±4.09	103.68±8.17
	150	143.11±0.11	152.92±5.89	101.94±3.93
Saen Saeb canal	0	0.64±0.06	ND	-
	25	24.66±0.14	25.34±0.90	101.36±3.63
	50	45.72±0.23	47.67±3.02	95.34±6.05
	150	146.48±0.26	153.77±5.31	102.51±3.54

CHAPTER V
CONCLUSIONS

5.1 Conclusions

In this study, G/PANI/PS nanoporous fiber modified SPCE was successfully prepared via electrospinning fabrication. The high surface area and high conductivity of electrospun G/PANI/PS nanoporous fiber significantly improved the electrochemical sensitivity in the detection of standard $Fe[(CN)_6]^{3-/4-}$ redox couple and heavy metals (*e.g.* Pb^{2+} and Cd^{2+}).

For the fabrication of G/PANI/PS nanoporous fiber modified SPCE, the optimal conditions include 20% w/v of PS, 10.5 kV of applied voltage, 0.5 mL/h of flow rate, and 15 cm of needle tip-to collector.

The optimal parameters of square wave anodic stirpping voltammetry (SWASV) for heavy metal detection include HCl as a supporting electrolyte (pH of 1.0), a Bi^{3+} concentration of 900 μg L^{-1}, a deposition potential of -1.2 V, a deposition time of 180 s, a frequency of 100 Hz, a potential amplitude of 40 mV, and a step potential of 21 mV. The electrospun G/PANI/PS nanoporous fiber provide the high electrochemical sensitivity (8-fold for Cd^{2+} and 5 fold for Pb^{2+} compared with an unmodified carbon electrode). The calibration cure was obtained in a linear range of 10-500 μg L^{-1} with a correlation coefficient (R^2) of 0.992 and 0.991 for Pb^{2+} and Cd^{2+}, respectively. The limit of detection (LOD) was found to be 3.30 μg L^{-1} for Pb^{2+} and 4.43 μg L^{-1} for Cd^{2+} and the limit of quantitation (LOQ) was found to be 11.02 μg L^{-1} for Pb^{2+} and 14.78 μg L^{-1} for Cd^{2+}. Moreover, this developed system can be used repeatedly for more than 10 times with 4.67% RSD for Pb^{2+} and 3.52% RSD for Cd^{2+}.

To validate and evaluate this proposed system, G/PANI/PS nanoporous fiber modified electrode was applied to measure Pb^{2+} and Cd^{2+} in the real river water samples and compared with ICP-OES technique. The % recoveries were found in the range of 85-109% and 95-116% for Pb^{2+} and Cd^{2+}, respectively.

5.2 Suggestion for future work

A novel and sensitive electrode system based on G/PANI/PS nanoporous fiber developed in this study might be an alternative tool for various fields of applications, such as environmental monitoring, food inspection as well as medical diagnosis.

The electrospun fiber size and arrangement on the working electrode might be further investigated and optimized for improving the electrochemical sensitivity of modified electrode.

REFERENCES

[1] Yantasee, W., Charnhattakorn, B., Fryxell, G.E., Lin, Y., Timchalk, C., and Addleman, R.S. Detection of Cd, Pb, and Cu in non-pretreated natural waters and urine with thiol functionalized mesoporous silica and Nafion composite electrodes. Analytica Chimica Acta 620(1–2) (2008): 55-63.

[2] Ouyang, R., Zhu, Z., Tatum, C.E., Chambers, J.Q., and Xue, Z.-L. Simultaneous stripping detection of Zn(II), Cd(II) and Pb(II) using a bimetallic Hg–Bi/single-walled carbon nanotubes composite electrode. Journal of Electroanalytical Chemistry 656(1–2) (2011): 78-84.

[3] Jiang, L.-C. and Zhang, W.-D. A highly sensitive nonenzymatic glucose sensor based on CuO nanoparticles-modified carbon nanotube electrode. Biosensors and Bioelectronics 25(6) (2010): 1402-1407.

[4] Zheng, B., Liu, G., Yao, A., Xiao, Y., Du, J., Guo, Y., Xiao, D., Hu, Q., and Choi, M.M.F. A sensitive AgNPs/CuO nanofibers non-enzymatic glucose sensor based on electrospinning technology. Sensors and Actuators B: Chemical 195(0) (2014): 431-438.

[5] Hrapovic, S., Liu, Y., Male, K.B., and Luong, J.H.T. Electrochemical Biosensing Platforms Using Platinum Nanoparticles and Carbon Nanotubes. Analytical Chemistry 76(4) (2003): 1083-1088.

[6] Huang, J., Liu, Y., Hou, H., and You, T. Simultaneous electrochemical determination of dopamine, uric acid and ascorbic acid using palladium nanoparticle-loaded carbon nanofibers modified electrode. Biosensors and Bioelectronics 24(4) (2008): 632-637.

[7] Kuila, T., Bose, S., Khanra, P., Mishra, A.K., Kim, N.H., and Lee, J.H. Recent advances in graphene-based biosensors. Biosensors and Bioelectronics 26(12) (2011): 4637-4648.

[8] Aragay, G. and Merkoçi, A. Nanomaterials application in electrochemical detection of heavy metals. Electrochimica Acta 84(0) (2012): 49-61.

[9] Zhou, Z. and Wu, X.-F. Graphene-beaded carbon nanofibers for use in supercapacitor electrodes: Synthesis and electrochemical characterization. Journal of Power Sources 222(0) (2013): 410-416.

[10] Wang, Z. and Liu, E. Graphene ultrathin film electrode for detection of lead ions in acetate buffer solution. Talanta 103(0) (2013): 47-55.

[11] Bhadra, S., Khastgir, D., Singha, N.K., and Lee, J.H. Progress in preparation, processing and applications of polyaniline. Progress in Polymer Science 34(8) (2009): 783-810.

[12] Chen, L., Su, Z., He, X., Liu, Y., Qin, C., Zhou, Y., Li, Z., Wang, L., Xie, Q., and Yao, S. Square wave anodic stripping voltammetric determination of Cd and Pb ions at a Bi/Nafion/thiolated polyaniline/glassy carbon electrode. Electrochemistry Communications 15(1) (2012): 34-37.

[13] Fan, Y., Liu, J.-H., Yang, C.-P., Yu, M., and Liu, P. Graphene–polyaniline composite film modified electrode for voltammetric determination of 4-aminophenol. Sensors and Actuators B: Chemical 157(2) (2011): 669-674.

[14] Rodthongkum, N., Ruecha, N., Rangkupan, R., Vachet, R.W., and Chailapakul, O. Graphene-loaded nanofiber-modified electrodes for the ultrasensitive determination of dopamine. Analytica Chimica Acta 804(0) (2013): 84-91.

[15] Ruecha, N., Rangkupan, R., Rodthongkum, N., and Chailapakul, O. Novel paper-based cholesterol biosensor using graphene/polyvinylpyrrolidone/polyaniline nanocomposite. Biosens Bioelectron 52 (2014): 13-9.

[16] Sundaray, B., Choi, A., and Park, Y.W. Highly conducting electrospun polyaniline-polyethylene oxide nanofibrous membranes filled with single-walled carbon nanotubes. Synthetic Metals 160(9–10) (2010): 984-988.

[17] Wang, H., Yang, P.-H., Cai, H.-H., and Cai, J. Constructions of polyaniline nanofiber-based electrochemical sensor for specific detection of nitrite and sensitive monitoring of ascorbic acid scavenging nitrite. Synthetic Metals 162(3-4) (2012): 326-331.

[18] Wang, Z., Liu, E., and Zhao, X. Glassy carbon electrode modified by conductive polyaniline coating for determination of trace lead and cadmium ions in acetate buffer solution. Thin Solid Films 519(15) (2011): 5285-5289.

[19] Zhai, G., Fan, Q., Tang, Y., Zhang, Y., Pan, D., and Qin, Z. Conductive composite films composed of polyaniline thin layers on microporous polyacrylonitrile surfaces. Thin Solid Films 519(1) (2010): 169-173.

[20] Cesarino, I., Galesco, H.V., and Machado, S.A.S. Determination of serotonin on platinum electrode modified with carbon nanotubes/polypyrrole/silver nanoparticles nanohybrid. Materials Science and Engineering: C 40(0) (2014): 49-54.

[21] Qian, T., Yu, C., Zhou, X., Wu, S., and Shen, J. Au nanoparticles decorated polypyrrole/reduced graphene oxide hybrid sheets for ultrasensitive dopamine detection. Sensors and Actuators B: Chemical 193(0) (2014): 759-763.

[22] Wei, Y., Yang, R., Liu, J.-H., and Huang, X.-J. Selective detection toward Hg(II) and Pb(II) using polypyrrole/carbonaceous nanospheres modified screen-printed electrode. Electrochimica Acta 105(0) (2013): 218-223.

[23] Bianchini, C., Curulli, A., Pasquali, M., and Zane, D. Determination of caffeic acid in wine using PEDOT film modified electrode. Food Chem 156(0) (2014): 81-86.

[24] Wisitsoraat, A., Pakapongpan, S., Sriprachuabwong, C., Phokharatkul, D., Sritongkham, P., Lomas, T., and Tuantranont, A. Graphene–PEDOT:PSS on screen printed carbon electrode for enzymatic biosensing. Journal of Electroanalytical Chemistry 704(0) (2013): 208-213.

[25] Radhakrishnan, S., Sumathi, C., Umar, A., Jae Kim, S., Wilson, J., and Dharuman, V. Polypyrrole–poly(3,4-ethylenedioxythiophene)–Ag (PPy–PEDOT–Ag) nanocomposite films for label-free electrochemical DNA sensing. Biosensors and Bioelectronics 47(0) (2013): 133-140.

[26] Guimard, N.K., Gomez, N., and Schmidt, C.E. Conducting polymers in biomedical engineering. Progress in Polymer Science 32(8–9) (2007): 876-921.

[27] Matsumoto, H. and Tanioka, A. Functionality in Electrospun Nanofibrous Membranes Based on Fiber's Size, Surface Area, and Molecular Orientation. Membranes 1(3) (2011): 249-264.

[28] Fashandi, H. and Karimi, M. Pore formation in polystyrene fiber by superimposing temperature and relative humidity of electrospinning atmosphere. Polymer 53(25) (2012): 5832-5849.

[29] Bhardwaj, N. and Kundu, S.C. Electrospinning: A fascinating fiber fabrication technique. Biotechnology Advances 28(3) (2010): 325-347.

[30] Ding, B., Wang, M., Wang, X., Yu, J., and Sun, G. Electrospun nanomaterials for ultrasensitive sensors. Materials Today 13(11) (2010): 16-27.

[31] Marx, S., Jose, M.V., Andersen, J.D., and Russell, A.J. Electrospun gold nanofiber electrodes for biosensors. Biosensors and Bioelectronics 26(6) (2011): 2981-2986.

[32] Scampicchio, M., Arecchi, A., Bianco, A., Bulbarello, A., Bertarelli, C., and Mannino, S. Nylon Nanofibrous Biosensors for Glucose Determination. Electroanalysis 22(10) (2010): 1056-1060.

[33] Bao, Q., Zhang, H., Yang, J.-x., Wang, S., Tang, D.Y., Jose, R., Ramakrishna, S., Lim, C.T., and Loh, K.P. Graphene–Polymer Nanofiber Membrane for Ultrafast Photonics. Advanced Functional Materials 20(5) (2010): 782-791.

[34] Zhu, H., Du, M., Zhang, M., Wang, P., Bao, S., Fu, Y., and Yao, J. Facile and green fabrication of small, mono-disperse and size-controlled noble metal nanoparticles embedded in water-stable polyvinyl alcohol nanofibers: High sensitive, flexible and reliable materials for biosensors. Sensors and Actuators B: Chemical 185(0) (2013): 608-619.

[35] Afkhami, A., Ghaedi, H., Madrakian, T., and Rezaeivala, M. Highly sensitive simultaneous electrochemical determination of trace amounts of Pb(II) and Cd(II) using a carbon paste electrode modified with multi-walled carbon nanotubes and a newly synthesized Schiff base. Electrochimica Acta 89 (2013): 377-386.

[36] Chen, J. and Teo, K.C. Determination of cadmium, copper, lead and zinc in water samples by flame atomic absorption spectrometry after cloud point extraction. Analytica Chimica Acta 450(1–2) (2001): 215-222.

[37] Palmer, C.D., Lewis Jr, M.E., Geraghty, C.M., Barbosa Jr, F., and Parsons, P.J. Determination of lead, cadmium and mercury in blood for assessment of environmental exposure: A comparison between inductively coupled plasma–mass spectrometry and atomic absorption spectrometry. Spectrochimica Acta Part B: Atomic Spectroscopy 61(8) (2006): 980-990.

[38] Schramel, P., Wendler, I., and Angerer, J. The determination of metals (antimony, bismuth, lead, cadmium, mercury, palladium, platinum, tellurium, thallium, tin and tungsten) in urine samples by inductively coupled plasma-mass spectrometry. International Archives of Occupational and Environmental Health 69(3) (1997): 219-223.

[39] Zhang, Z.-W., Shimbo, S., Ochi, N., Eguchi, M., Watanabe, T., Moon, C.-S., and Ikeda, M. Determination of lead and cadmium in food and blood by inductively coupled plasma mass spectrometry: a comparison with graphite furnace atomic absorption spectrometry. Science of The Total Environment 205(2–3) (1997): 179-187.

[40] Pyle, S.M., Nocerino, J.M., Deming, S.N., Palasota, J.A., Palasota, J.M., Miller, E.L., Hillman, D.C., Kuharic, C.A., Cole, W.H., Fitzpatrick, P.M., Watson, M.A., and Nichols, K.D. Comparison of AAS, ICP-AES, PSA, and XRF in Determining Lead and Cadmium in Soil. Environmental Science & Technology 30(1) (1995): 204-213.

[41] Lv, M., Wang, X., Li, J., Yang, X., Zhang, C.a., Yang, J., and Hu, H. Cyclodextrin-reduced graphene oxide hybrid nanosheets for the simultaneous determination of lead(II) and cadmium(II) using square wave anodic stripping voltammetry. Electrochimica Acta 108(0) (2013): 412-420.

[42] Kempegowda, R.G. and Malingappa, P. A binderless, covalently bulk modified electrochemical sensor: application to simultaneous determination of lead and cadmium at trace level. Analytica Chimica Acta 728 (2012): 9-17.

[43] Guell, R., Aragay, G., Fontas, C., Antico, E., and Merkoci, A. Sensitive and stable monitoring of lead and cadmium in seawater using screen-printed electrode and electrochemical stripping analysis. Analytica Chimica Acta 627(2) (2008): 219-24.

[44] Chen, C., Niu, X., Chai, Y., Zhao, H., and Lan, M. Bismuth-based porous screen-printed carbon electrode with enhanced sensitivity for trace heavy metal detection by stripping voltammetry. Sensors and Actuators B: Chemical 178(0) (2013): 339-342.

[45] Keawkim, K., Chuanuwatanakul, S., Chailapakul, O., and Motomizu, S. Determination of lead and cadmium in rice samples by sequential injection/anodic stripping voltammetry using a bismuth film/crown ether/Nafion modified screen-printed carbon electrode. Food Control 31(1) (2013): 14-21.

[46] Lezi, N., Economou, A., Dimovasilis, P.A., Trikalitis, P.N., and Prodromidis, M.I. Disposable screen-printed sensors modified with bismuth precursor compounds for the rapid voltammetric screening of trace Pb(II) and Cd(II). Analytica Chimica Acta 728(0) (2012): 1-8.

[47] Wang, J. Analytical Electrochemistry. 2 ed. the United staes of America: Wiley-VCH, 2000.

[48] Bard, A.J. and Faulkner, L.R. Electrochemical methods : fundamentals and applications, ed. 2. the United States of America: John Wiley & Sons, Inc, 2001.

[49] Carlos, M.P. and Rubin, G. Electroanalytical Techniques and Instrumentation in Food Analysis. in Handbook of Food Analysis Instruments: CRC Press, 2008.

[50] Lü, M., Li, J., Yang, X., Zhang, C., Yang, J., Hu, H., and Wang, X. Applications of graphene-based materials in environmental protection and detection. Chinese Science Bulletin 58(22) (2013): 2698-2710.

[51] Wang, C., Li, D., Too, C.O., and Wallace, G.G. Electrochemical Properties of Graphene Paper Electrodes Used in Lithium Batteries. Chemistry of Materials 21(13) (2009): 2604-2606.

[52] Md. Aminur Rahman , P.K., Deog-Su Park and Yoon-Bo Shim Electrochemical Sensors Based on Organic Conjugated Polymers. Sensors 8(1) (2008): 118-141.

[53] Xue, H., Shen, Z., and Li, C. Improved selectivity and stability of glucose biosensor based on in situ electropolymerized polyaniline-polyacrylonitrile composite film. Biosensors and Bioelectronics 20(11) (2005): 2330-4.

[54] Chronakis, I.S., Grapenson, S., and Jakob, A. Conductive polypyrrole nanofibers via electrospinning: Electrical and morphological properties. Polymer 47(5) (2006): 1597-1603.

[55] Xu, J., Zhang, H., and Chen, G. Carbon nanotube/polystyrene composite electrode for microchip electrophoretic determination of rutin and quercetin in Flos Sophorae Immaturus. Talanta 73(5) (2007): 932-7.

[56] Khaskheli, A.R., Fischer, J., Barek, J., Vyskočil, V., Sirajuddin, and Bhanger, M.I. Differential pulse voltammetric determination of paracetamol in tablet and urine samples at a micro-crystalline natural graphite–polystyrene composite film modified electrode. Electrochimica Acta 101 (2013): 238-242.

[57] Qian, T., Yu, C., Wu, S., and Shen, J. Gold nanoparticles coated polystyrene/reduced graphite oxide microspheres with improved dispersibility and electrical conductivity for dopamine detection. Colloids and Surfaces B: Biointerfaces 112 (2013): 310-4.

[58] Economou, A. Bismuth-film electrodes: recent developments and potentialities for electroanalysis. TrAC Trends in Analytical Chemistry 24(4) (2005): 334-340.

[59] Arduini, F., Calvo, J.Q., Palleschi, G., Moscone, D., and Amine, A. Bismuth-modified electrodes for lead detection. TrAC Trends in Analytical Chemistry 29(11) (2010): 1295-1304.

[60] Wang, J. Stripping Analysis at Bismuth Electrodes: A Review. Electroanalysis 17(15-16) (2005): 1341-1346.

[61] Wonsawat, W., Chuanuwatanakul, S., Dungchai, W., Punrat, E., Motomizu, S., and Chailapakul, O. Graphene-carbon paste electrode for cadmium and lead ion monitoring in a flow-based system. Talanta 100 (2012): 282-9.

[62] Yu, X., Xiang, H., Long, Y., Zhao, N., Zhang, X., and Xu, J. Preparation of porous polyacrylonitrile fibers by electrospinning a ternary system of PAN/DMF/H2O. Materials Letters 64(22) (2010): 2407-2409.

[63] Laurencin, C.T., Kumbar, S.G., Nukavarapu, S.P., James, R., and Hogan, M.V. Recent Patents on Electrospun Biomedical Nanostructures: An Overview. Recent Patents on Biomedical Engineering 1(1) (2008): 68-78.

[64] Reneker, D.H., Yarin, A.L., Fong, H., and Koombhongse, S. Bending instability of electrically charged liquid jets of polymer solutions in electrospinning. Journal of Applied Physics 87(9) (2000): 4531-4547.

[65] Andrady, A.L. Introduction. in Science and Technology of Polymer Nanofibers, pp. 1-26: John Wiley & Sons, Inc., 2007.

[66] Rangkupan, R. and Reneker, D.H. Electrospinning Process of Molten Polypropylene in Vacuum Journal of Metals, Materials and Minerals 12(2) (2003): 81-87.

[67] Teo, W.-E. Electrospinning Basics - Jet Initiation [online]. 2013. Available from: http://electrospintech.com/jet-initiation.html#.VEZ5WSKUe0V [20 October 2014]

[68] Garg, K. and Bowlin, G.L. Electrospinning jets and nanofibrous structures. Biomicrofluidics 5(1) (2011): 13403.

[69] Andrady, A.L. Factors Affecting Nanofiber Quality. in Science and Technology of Polymer Nanofibers, pp. 81-110: John Wiley & Sons, Inc., 2007.

[70] Subbiah, T., Bhat, G.S., Tock, R.W., Parameswaran, S., and Ramkumar, S.S. Electrospinning of nanofibers. Journal of Applied Polymer Science 96(2) (2005): 557-569.

[71] Jarusuwannapoom, T., Hongrojjanawiwat, W., Jitjaicham, S., Wannatong, L., Nithitanakul, M., Pattamaprom, C., Koombhongse, P., Rangkupan, R., and Supaphol, P. Effect of solvents on electro-spinnability of polystyrene solutions and morphological appearance of resulting electrospun polystyrene fibers. European Polymer Journal 41(3) (2005): 409-421.

[72] Wannatong, L., Sirivat, A., and Supaphol, P. Effects of solvents on electrospun polymeric fibers: preliminary study on polystyrene. Polymer International 53(11) (2004): 1851-1859.

[73] Kedem, S., Schmidt, J., Paz, Y., and Cohen, Y. Composite Polymer Nanofibers with Carbon Nanotubes and Titanium Dioxide Particles. Langmuir 21 (2005): 5600-5604.

[74] Hsu, C.-M. and Shivkumar, S. Nano-sized beads and porous fiber constructs of Poly(**ε**-caprolactone) produced by electrospinning. Journal of Materials Science 39(9) (2004): 3003-3013.

[75] Shin, M.K., Kim, Y.J., Kim, S.I., Kim, S.-K., Lee, H., Spinks, G.M., and Kim, S.J. Enhanced conductivity of aligned PANi/PEO/MWNT nanofibers by electrospinning. Sensors and Actuators B: Chemical 134(1) (2008): 122-126.

[76] Casper, C.L., Stephens, J.S., Tassi, N.G., Chase, D.B., and Rabolt, J.F. Controlling Surface Morphology of Electrospun Polystyrene Fibers: Effect of Humidity and Molecular Weight in the Electrospinning Process. Macromolecules 37(2) (2003): 573-578.

[77] Megelski, S., Stephens, J.S., Chase, D.B., and Rabolt, J.F. Micro- and Nanostructured Surface Morphology on Electrospun Polymer Fibers. Macromolecules 35(22) (2002): 8456-8466.

[78] World Health Organization. Lead in Drinking-water [online]. 2011. Available from: http://www.who.int/water_sanitation_health/dwq/chemicals/lead.pdf [2 November 2014]

[79] Duruibe, J.O., Ogwuegbu, M.O.C., and Egwurugwu, J.N. Heavy metal pollution and human biotoxic effects. International Journal of Physical Sciences 2(5) (2007): 112-118.

[80] Board, N.o.t.N.E. the Enhancement and Conservation of National Environmental Quality Act B.E.2535 (1992) [online]. B.E. 2537 (1994). Available from: http://www.pcd.go.th/info_serv/en_reg_std_water05.html

[81] Nguyen, P.K.Q. and Lunsford, S.K. Square wave anodic stripping voltammetric analysis of lead and cadmium utilizing titanium dioxide/zirconium dioxide carbon paste composite electrode. Journal of Electroanalytical Chemistry 711 (2013): 45-52.

[82] Ping, J., Wang, Y., Wu, J., and Ying, Y. Development of an electrochemically reduced graphene oxide modified disposable bismuth film electrode and its application for stripping analysis of heavy metals in milk. Food Chemistry 151 (2014): 65-71.

[83] Hwang, G.H., Han, W.K., Park, J.S., and Kang, S.G. Determination of trace metals by anodic stripping voltammetry using a bismuth-modified carbon nanotube electrode. Talanta 76(2) (2008): 301-308.

[84] Philips, M.F., Gopalan, A.I., and Lee, K.P. Development of a novel cyano group containing electrochemically deposited polymer film for ultrasensitive simultaneous detection of trace level cadmium and lead. Journal of Hazardous Materials 237-238 (2012): 46-54.

[85] Hu, C. Simultaneous determination of lead(II) and cadmium(II) at a diacetyldioxime modified carbon paste electrode by differential pulse stripping voltammetry. Talanta 60(1) (2003): 17-24.

[86] Wang, J., Lu, J., Kirgöz, Ü.A., Hocevar, S.B., and Ogorevc, B. Insights into the anodic stripping voltammetric behavior of bismuth film electrodes. Analytica Chimica Acta 434(1) (2001): 29-34.

VITA

Nadtinan Promphet was born in December 13, 1988 in Suratthani, Thailand. She received her Bachelor Degree of Science Program in Industrial chemistry from King Mongkut's Institute of Technology Ladkrabang, Bangkok, Thailand (2007-2011) and expect graduated her Master Degree of Science program in Petrochemical and Polymer Science from Chulalongkorn University, Bangkok, Thailand in 2014.

Poster presentations

Promphet, N., Rangkupan, R., Rattanarat, P., Thueploy, A., Rodthongkum, N., Chailapakul, O. "electrospun graphene/polyaniline modified carbon electrode for heavy metal detection" Pure and Applied Chemistry International Conference 2014 (PACCON2014), January 8-10, 2014, Khonkhen, Thailand.

Rodthongkum, N., Ruecha, N., Promphet, N., Rangkupan, R., Vachet, R.W., Chailapakul, O., Graphene-Loaded Nanofiber-Modified Electrode: A Novel and Sensitive Electrochemical Detection System. TechConnect World 2014, June 15-18, 2014, Washington DC, USA.

Proceedings

Promphet, N., Rangkupan, R., Rattanarat, P., Thueploy, A., Rodthongkum, N., Chailapakul, O. Electrospun graphene/polyaniline modified carbon electrode for heavy metal detection. Proceeding of Pure and Applied Chemistry International Conference 2014. 2014: 409-412.

Rodthongkum, N., Ruecha, N., Promphet, N., Rangkupan, R., Vachet, R.W., Chailapakul O., Graphene-Loaded Nanofiber-Modified Electrode: A Novel and Sensitive Electrochemical Detection System. Nanotech 2014.1(2014): 72-75.

Publications

Promphet, N., Rattanarat, P., Rangkupan, R., Chailapakul, O., Rodthongkum, N. An electrochemical sensor based on graphene/polyaniline/polystyrene nanoporous fibers modified electrode for simultaneous determination of lead and cadmium. Sensors and Actuators B: Chemical (impact factor: 3.84) 207 (2015): 526-534.